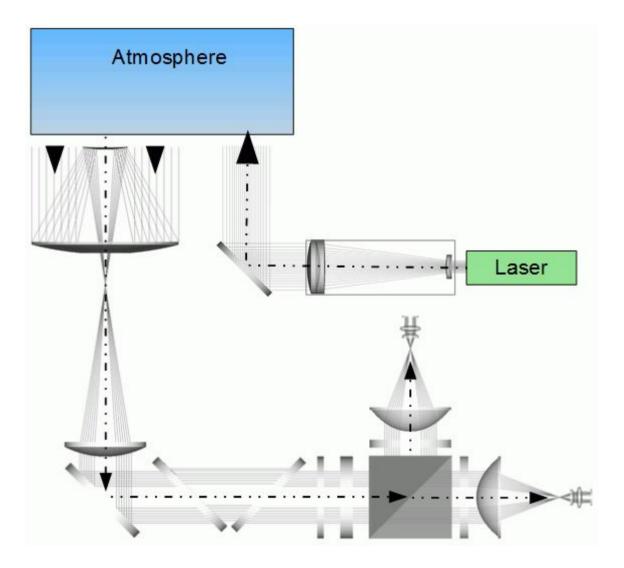
Basics of the lidar instrument: optics

Volker Freudenthaler

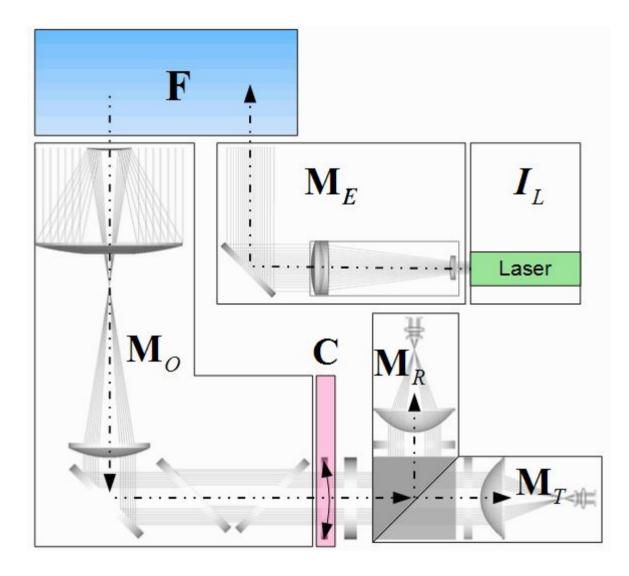
Meteorological Institute Ludwig-Maximilians University Munich, Germany

volker.freudenthaler@lmu.de

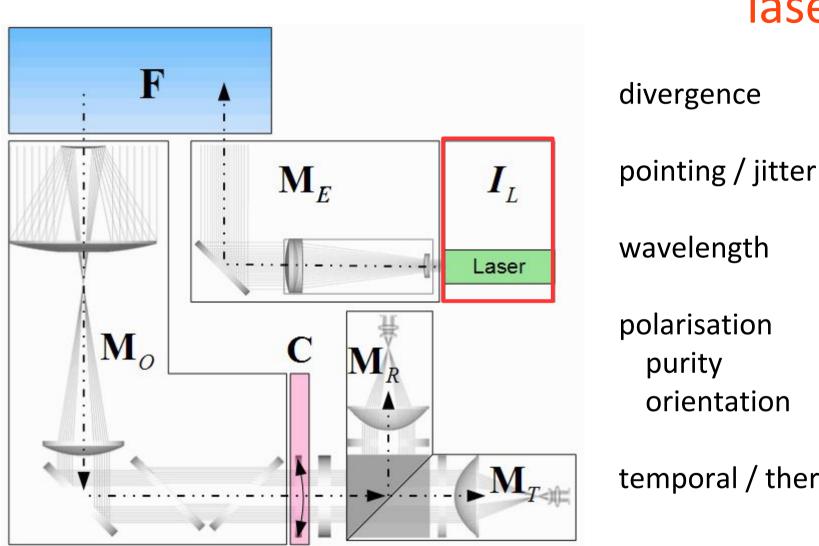








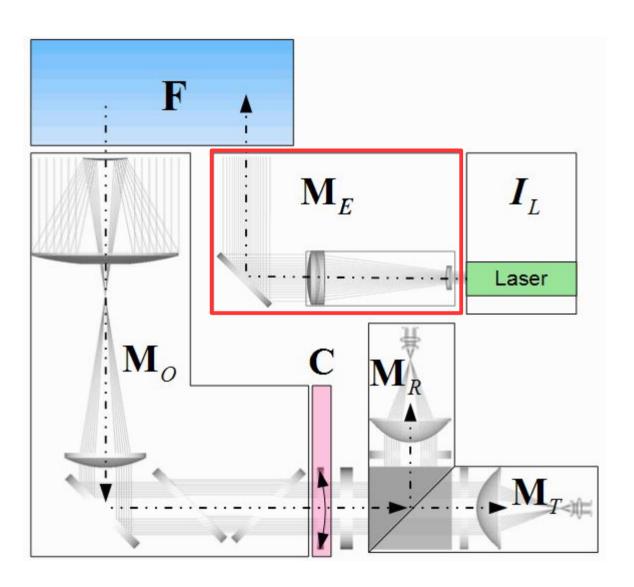




laser

temporal / thermal stability





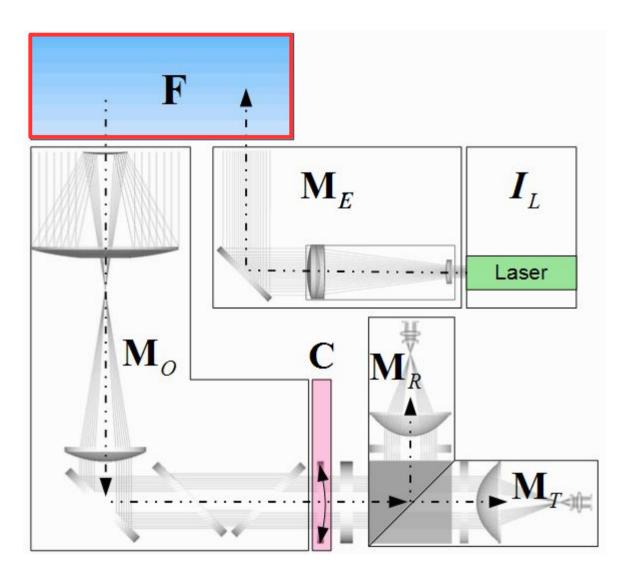
emitter and steering optics

wavelength dependent focus transmission polarisation birefringence

alignment accuracy stability alignment control

polarisation orientation flatness





atmosphere

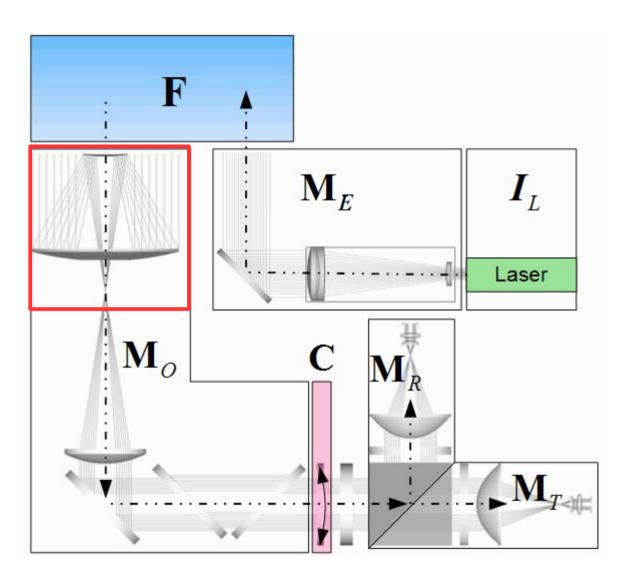
Rayleigh calibration

Rayleigh

backscatter coefficients depolarisation ratios Raman lines in IFF bw

radiosonde data





receiving optics telescope

focal length, diameter

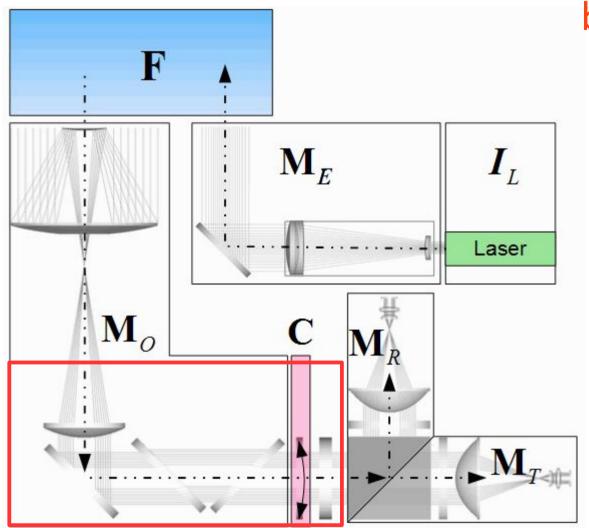
alignment stability

Newton telescope 90° mirror depolarisation

field of view



7



receiving optics beamsplitters and filters

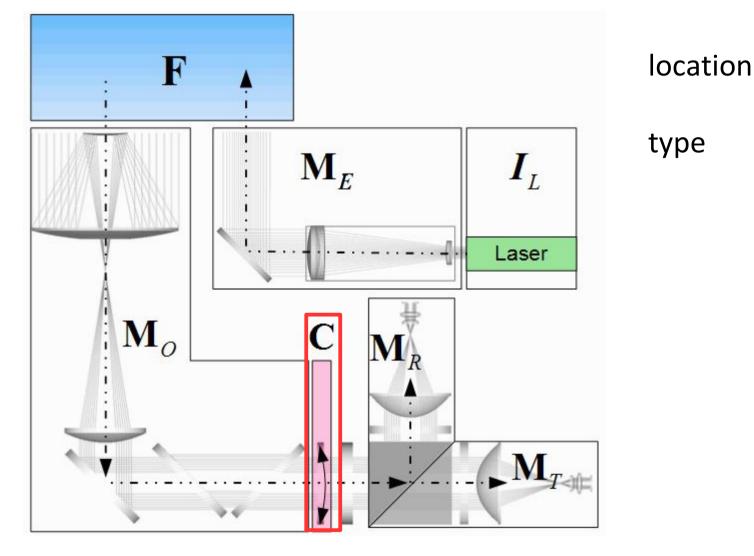
focal length of collimator => beam divergence => beam diameter

accpetance angles of beamsplitters and interference filters

polarisation problemes diattenuation retardance

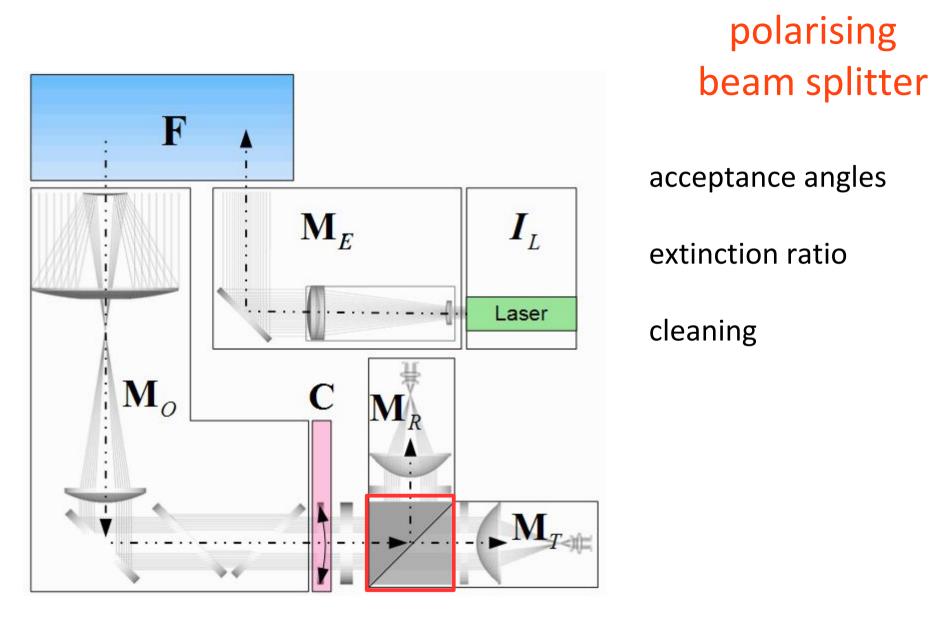


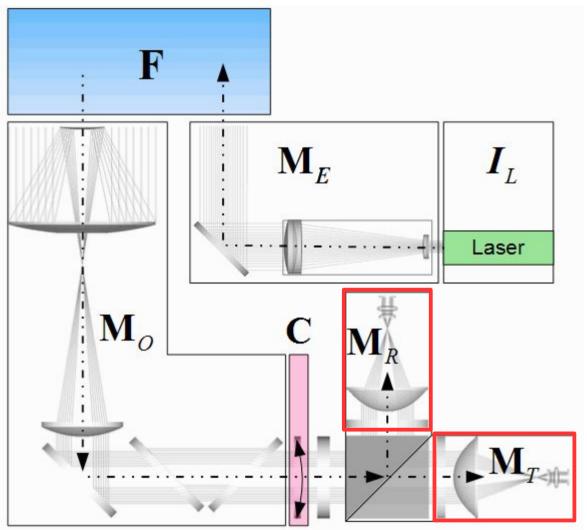




type







detectors and optics

PMT

homogeneity of the sensitivity

APD

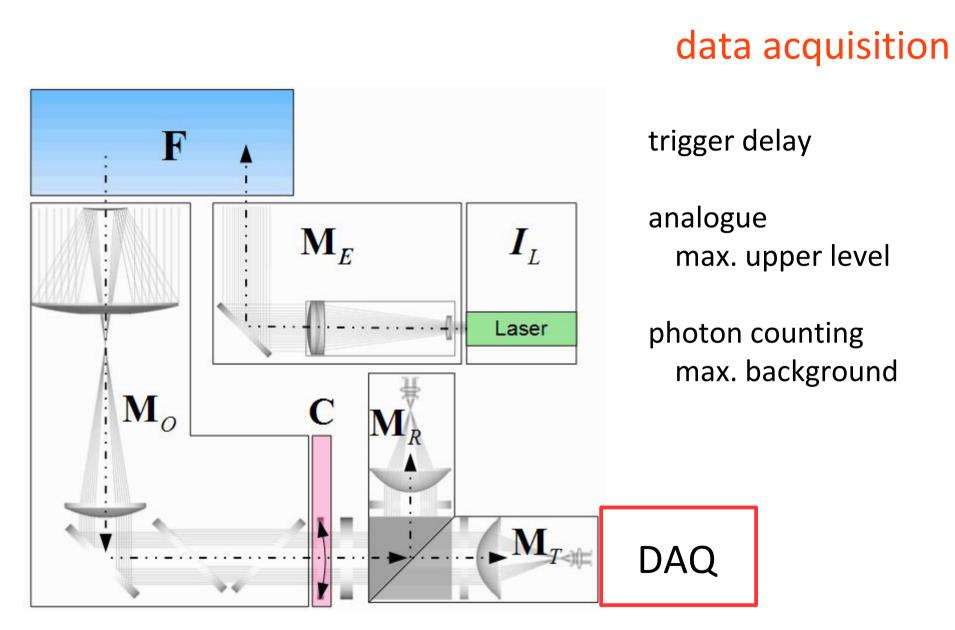
small diameter

eyepiece

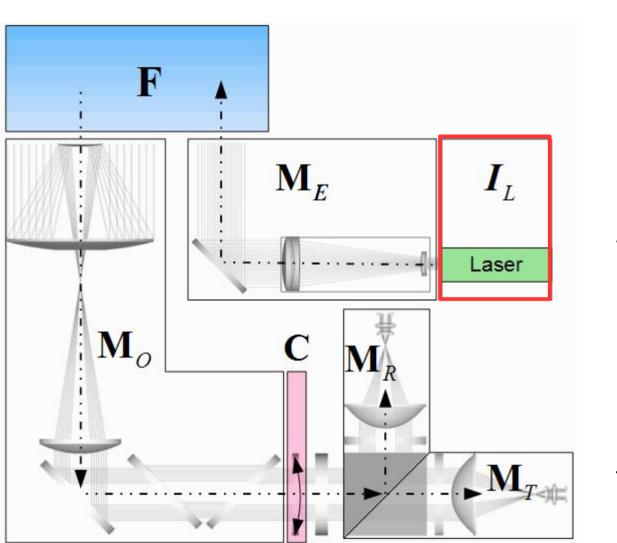
=> telescope imaging

neutral density filters
=> adjust signal level (LICEL)









laser

divergence pointing / jitter wavelength polarisation purity orientation

temporal / thermal stability



Brillant Specifications

Repetition rate (Hz)		10	10 SLM*	20	
Energy per pulse (mJ)	1064 nm	850	700	700	Measured with a calibrated wattmeter
	532 nm	400	290	300	
	355 nm	185/225	135	120/140	Regular/High energy UV option
	266 nm	90	60	60	
	213 nm	16	**	12	
Pointing stability (µrad)	1064 nm	<50	<50	<50	Measured by SPIRICON LBA-100,
	532 nm	<50	<50	<50	RMS, on 200 pulses at the focal plane
	355 nm	<50	<50	<50	of a 2m focus lens
	266 nm	<50	<50	<50	
Divergence (mrad)	1064 nm	0.5	0.5	0.55	Full angle, at 1/e ² of the peak, 85 % of total
-					energy
Polarization ratio (%)	1064 nm	>80	>70	>70	Horizontal polarization



source: http://www.quantel-laser.com

1D Gaußverteilung

$$f(x) = \frac{1}{\sqrt{2\pi\sigma}} \exp\left(-\frac{1}{2} \frac{(x-a)^2}{\sigma^2}\right)$$

2D symmetrische Gaußverteilung

Für $\rho = 0$ und $\sigma_1 = \sigma_2$

$$f(x_{1}, x_{2}) = \frac{1}{2\pi\sigma^{2}} \exp\left(-\frac{(x_{1} - a_{1})^{2} + (x_{2} - a_{2})^{2}}{2\sigma^{2}}\right)$$

$$r = \sqrt{x_{1}^{2} + x_{2}^{2}} \implies f(r) = \frac{1}{2\pi\sigma^{2}} \exp\left(-\frac{r^{2}}{2\sigma^{2}}\right)$$

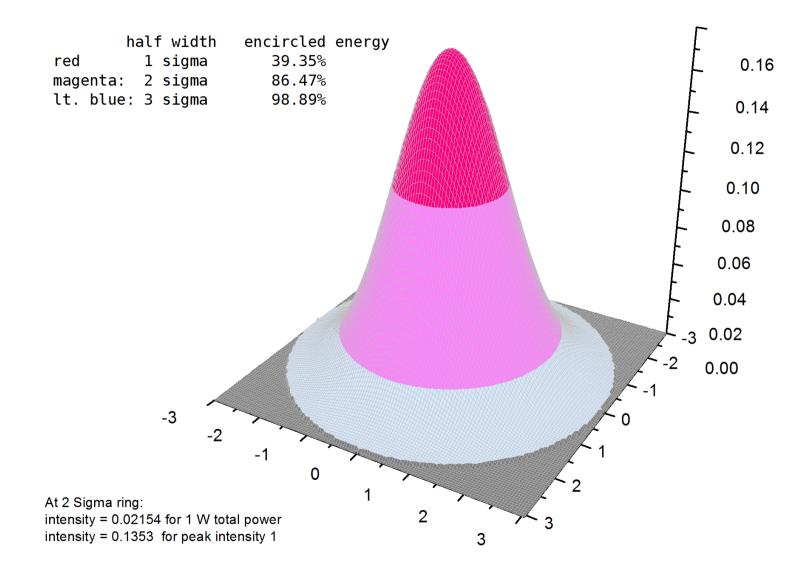
$$\int_{0}^{b} 2\pi r \cdot f(r) dr = \int_{0}^{b} \frac{r}{\sigma^{2}} \exp\left(-\frac{r^{2}}{2\sigma^{2}}\right) dr \text{ nicht analytisch lösbar.}$$

$$f(r)/f(0) = 0.5 \implies r_{1/2} = \sqrt{2\ln 2} \cdot \sigma \implies fwhm = 2r_{1/2} = 2.35482\sigma$$
Gaussian beam waist

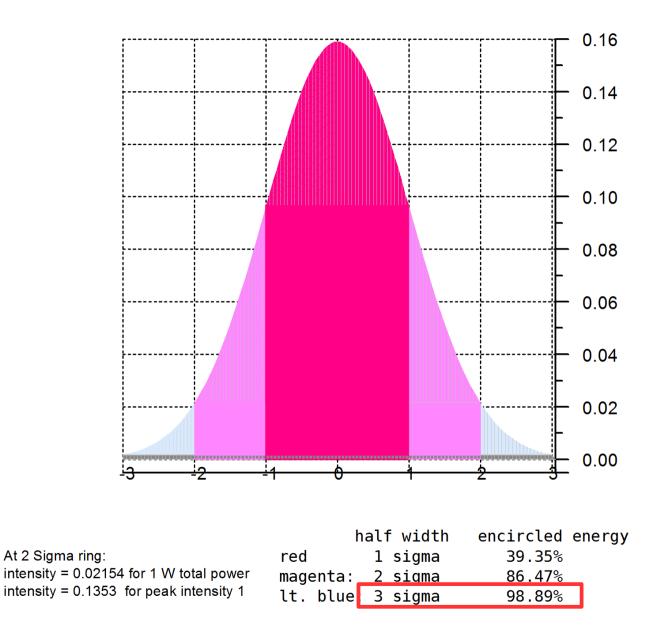
$$I(r,0) = \exp\left(-\frac{r^2}{2\sigma^2}\right) \Rightarrow \sigma = \frac{w}{2}$$



15



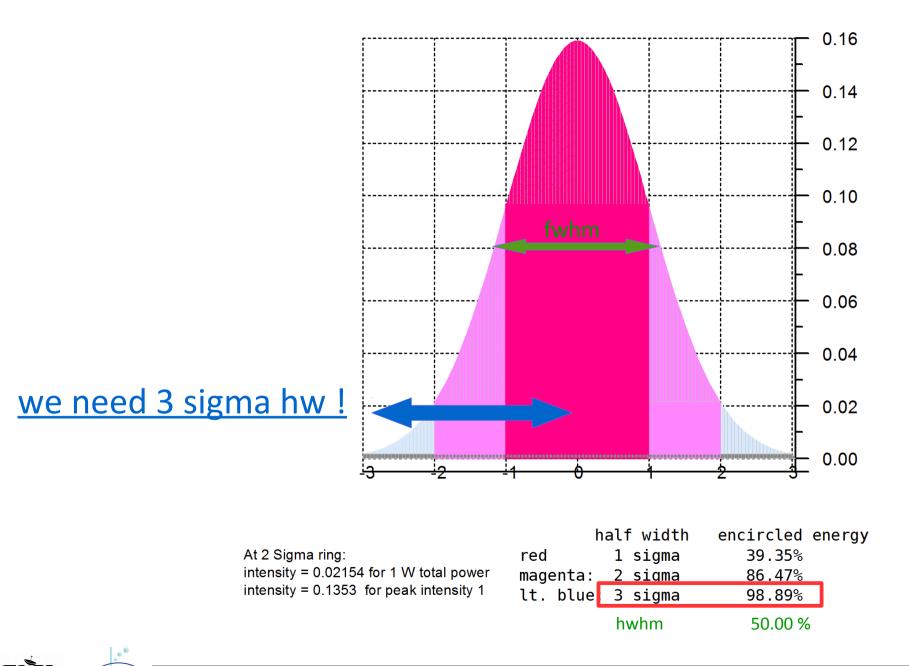






ACTRIS

Aerosol, Clouds and Trace gases Research InfraStructure



Brilliant Specifications

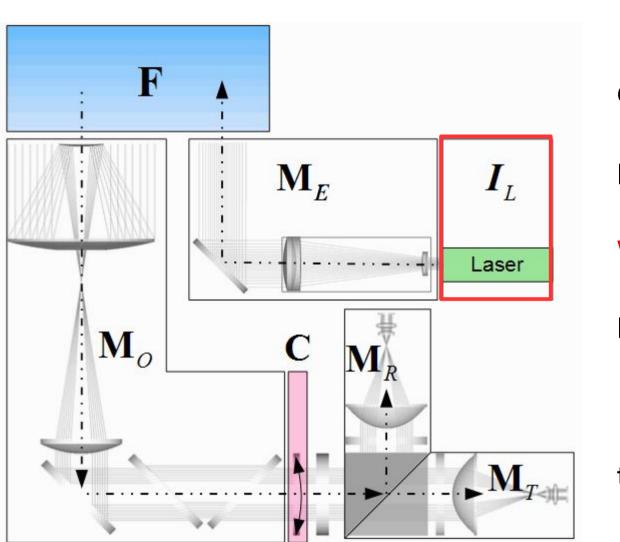
Repetition rate (Hz)		10	10 SLM*	20	
Energy per pulse (mJ)	1064 nm	850	700	700	Measured with a calibrated wattmeter
	532 nm	400	290	300	
	355 nm	185/225	135	120/140	Regular/High energy UV option
	266 nm	90	60	60	
	213 nm	16	**	12	
Pointing stability (µrad)	1064 nm	<50	<50	<50	Measured by SPIRICON LBA-100,
	532 nm	<50	<50	<50	RMS, on 200 pulses at the focal plane
	355 nm	<50	<50	<50	of a 2m focus lens
	266 nm	<50	<50	<50	
Divergence (mrad)	1064 nm	0.5	0.5	0.55	Full angle, at 1/e ² of the peak, 85 % of total
					energy
Polarization ratio (%)	1064 nm	>80	>70	>70	Horizontal polarization

3 sigma = 0.75 mrad pointing stability = 0.05 mrad (± ?)

beam fw = 0.85 mrad

source: http://www.quantel-laser.com





laser

divergence

pointing / jitter

wavelength

polarisation purity orientation

temporal / thermal stability



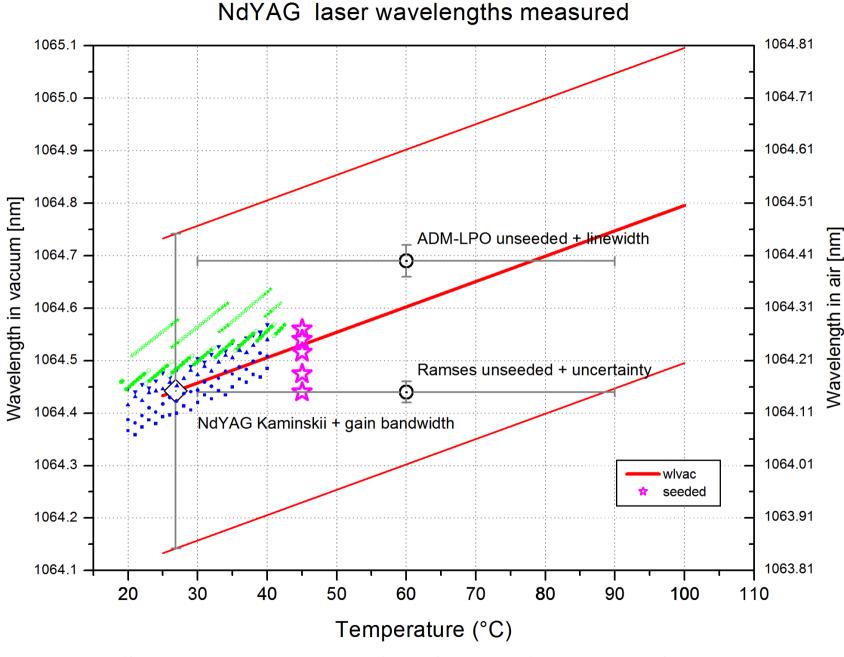
Brilliant Specifications

Repetition rate (Hz)		10	10 SLM*	20	
Energy per pulse (mJ)	1064 nm	850	700	700	Measured with a calibrated wattmeter
	532 nm	400	290	300	
	355 nm	185/225	135	120/140	Regular/High energy UV option
	266 nm	90	60	60	
	213 nm	16	**	12	
Pointing stability (µrad)	1064 nm	<50	<50	<50	Measured by SPIRICON LBA-100, RMS, on 200 pulses at the focal plane
	532 nm	<50	<50	<50	
	355 nm	<50	<50	<50	of a 2m focus lens
	266 nm	<50	<50	<50	
Divergence (mrad)	1064 nm	0.5	0.5	0.55	Full angle, at 1/e ² of the peak, 85 % of total
					energy
Polarization ratio (%)	1064 nm	>80	>70	>70	Horizontal polarization

Question: can we use an interference filter with 0.5 nm bandwidth ? (=> fwhm ?)



source: http://www.quantel-laser.com



source: http://www.meteo.physik.uni-muenchen.de/~stlidar/earlinet_asos/Rayleigh_scattering/Rayleigh_coefficients.pdf

East European Centre for Atmospheric Remote Sensing Research InfraStructure

Temperature and its distribution inside the NdYAG rod => laser design => environmental temperature => cooling stability

Laser gain bandwidth

Two laser lines

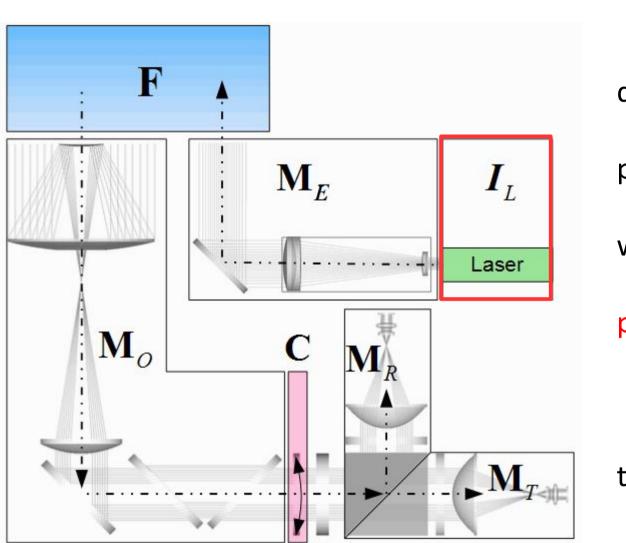
Theoretical and measurement uncertainties

The usual lidar laser is not of best quality (high price) => consider the worst case, unless verfied else.

Literature and references in => *Rayleigh coefficients ver1.4g.pdf*

http://www.meteo.physik.uni-muenchen.de/~stlidar/earlinet_asos/Rayleigh_scattering/Rayleigh_coefficients.pdf





laser

divergence

pointing / jitter

wavelength

polarisation purity orientation

temporal / thermal stability

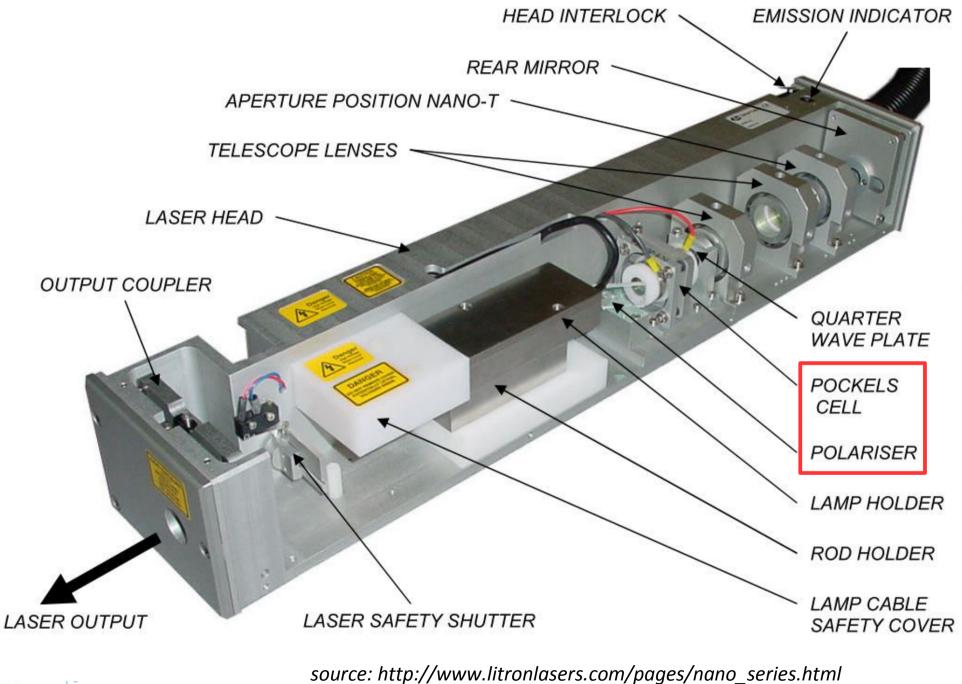


Brilliant Specifications

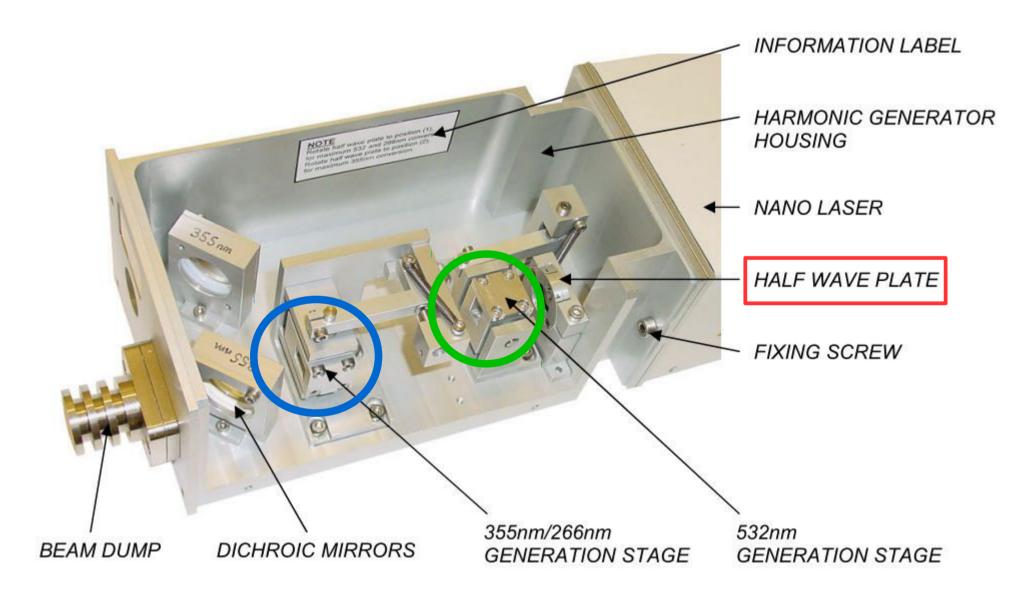
Repetition rate (Hz)		10	10 SLM*	20	
Energy per pulse (mJ)	1064 nm	850	700	700	Measured with a calibrated wattmeter
	532 nm	400	290	300	
	355 nm	185/225	135	120/140	Regular/High energy UV option
	266 nm	90	60	60	
	213 nm	16	**	12	
Pointing stability (µrad)	1064 nm	<50	<50	<50	Measured by SPIRICON LBA-100,
	532 nm	<50	<50	<50	RMS, on 200 pulses at the focal plane
	355 nm	<50	<50	<50	of a 2m focus lens
	266 nm	<50	<50	<50	
Divergence (mrad)	1064 nm	0.5	0.5	0.55	Full angle, at 1/e ² of the peak, 85 % of total
					energy
Polarization ratio (%)	1064 nm	<mark>>80</mark>	>70	>70	Horizontal polarization



source: http://www.quantel-laser.com







source: http://www.litronlasers.com/pages/nano_series.html



Linear polariser in the resonator should clean the 1064 polarisation,

- but NdYAG rod birefringence can decrease the DOLP (<u>Degree Of Linear Polarisation</u>) of 1064 nm
- SHG and THG only convert light in certain polarisation planes
 => DOLP of 355 should be very clean
 => DOLP of 532 could be decreased by THG
 => DOLP of the residual 1064 less than original

- Harmonic beam separators can decrease the DOLP

see also: https://en.wikipedia.org/wiki/Second-harmonic_generation https://www.rp-photonics.com/frequency_doubling.html



29

Giuseppe d'Amico 2006:

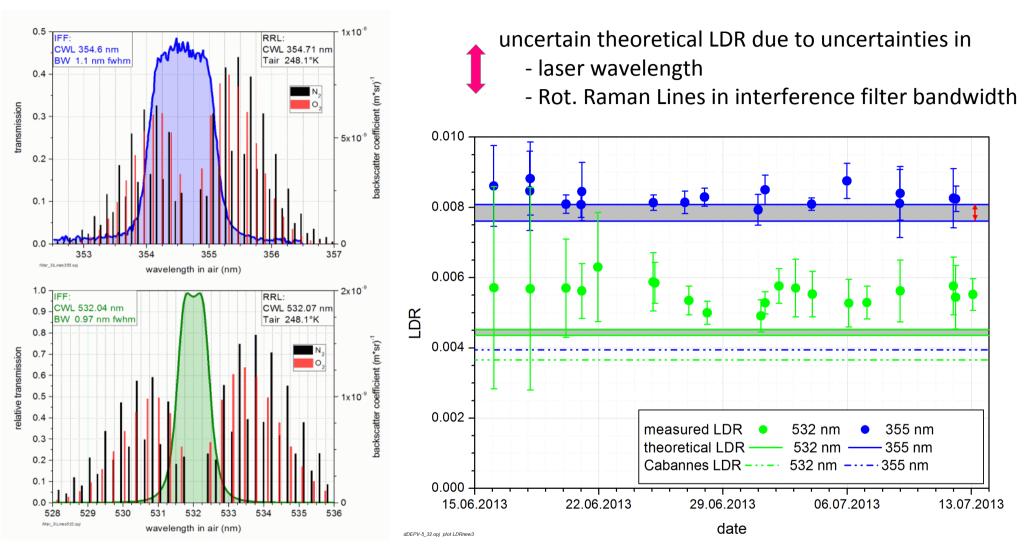
I send the measurement results from Continuum USA.

The measurements were done using a laser Surelite II - 10Hz with a SHG crystal of Type I and II. (so at 532 nm; Giuseppe)

Using both crystals, the energy of the vertical component of polarization was 3 Watts and the energy of the horizontal component was 2 mWatts corresponding to **polarization purity of about 99.93%**.

=> LDR = 0.002 / 3 = 0.00067

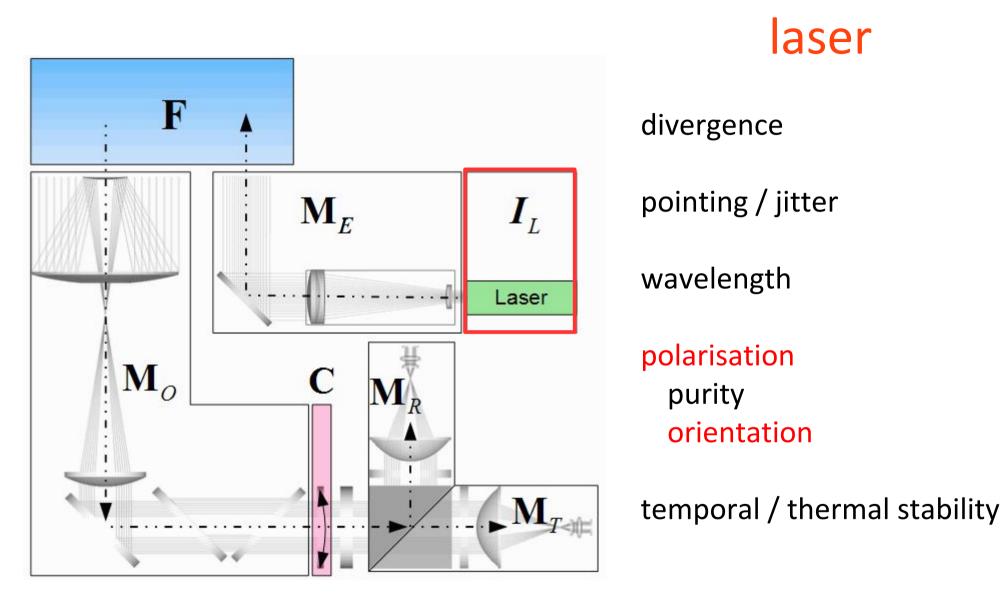




Laser polarisation must be cleaner than deviation of measurements from theory

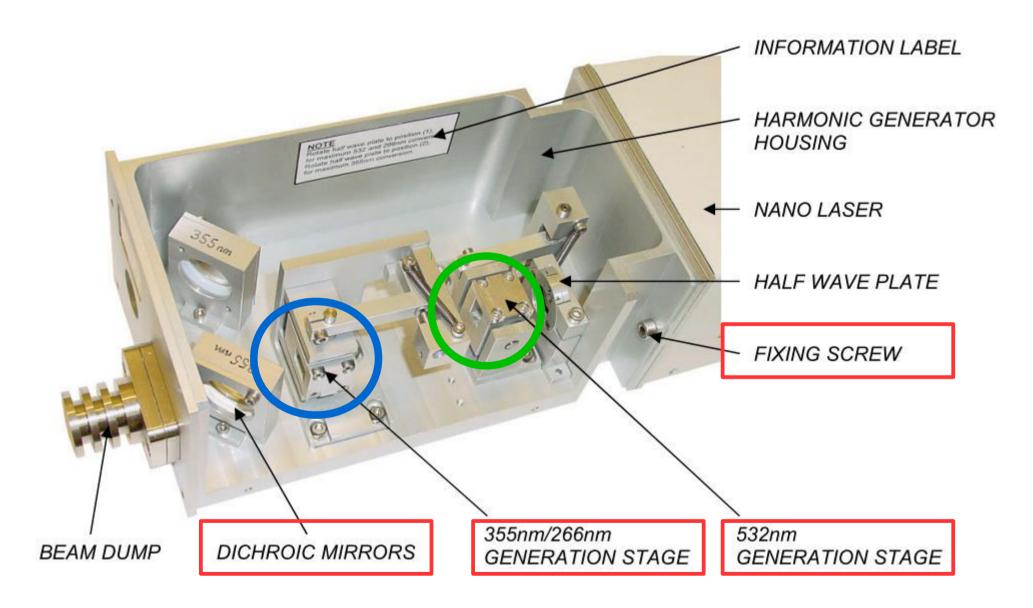
source: Freudenthaler et al., 27th ILRC 2015, Accuracy of linear depolaristion ratios in clear air ranges measured with POLIS-6 at 355 and 532 nm. https://epub.ub.uni-muenchen.de/24942/index.html

East European Centre for Atmospheric Remote Sension



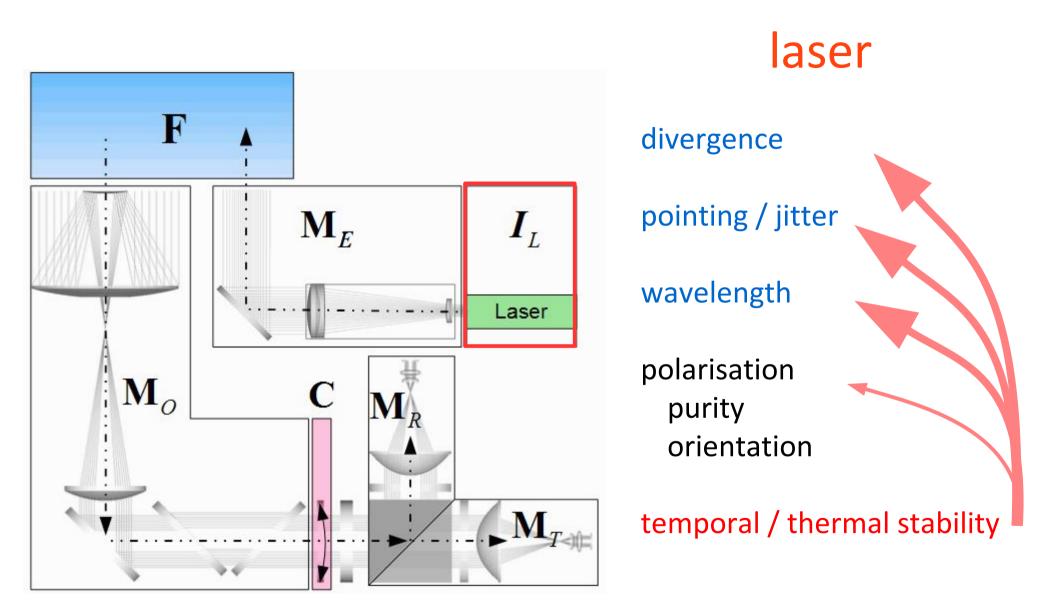
East European Centre for Atmospheric Remote Sensing

32

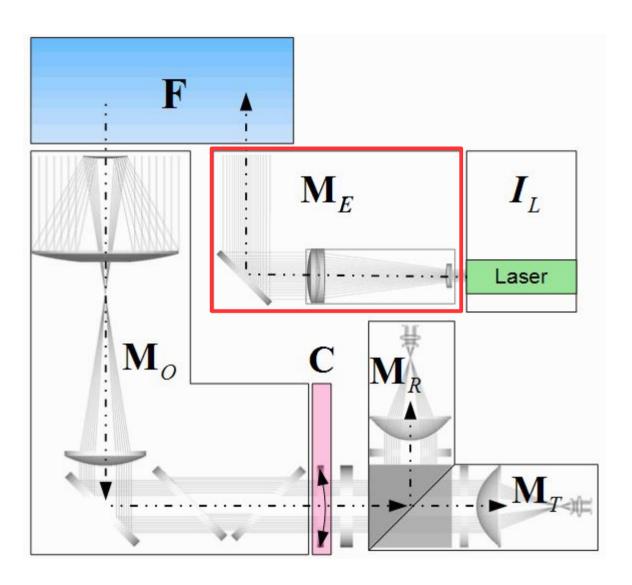


source: http://www.litronlasers.com/pages/nano_series.html









emitter and steering optics

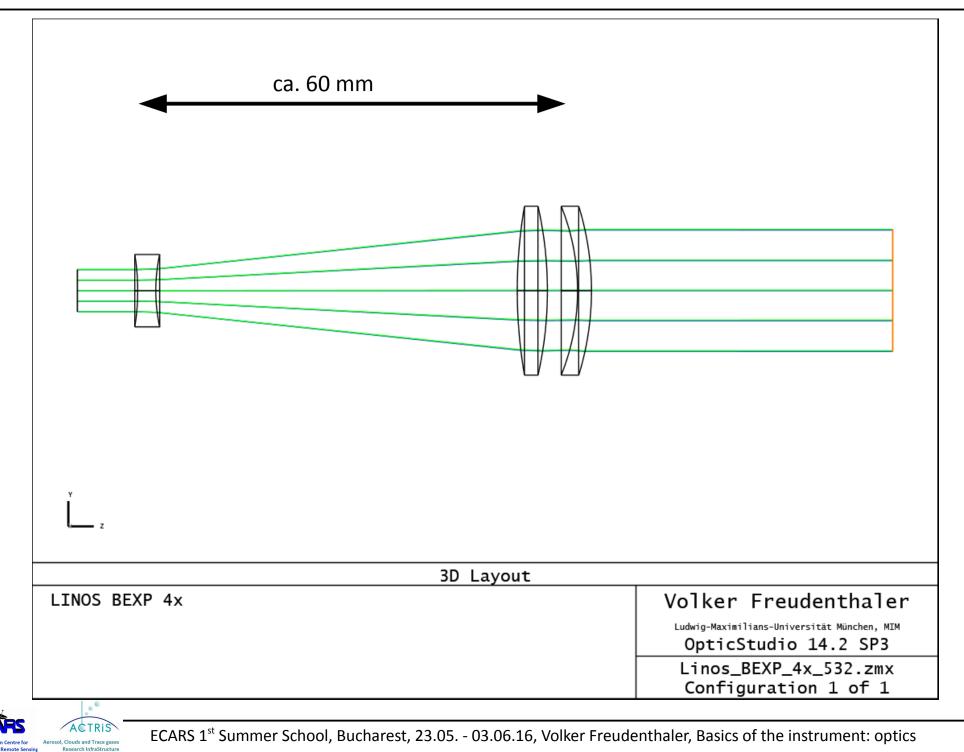
wavelength dependence
focal length => divergence
transmission
polarisation
birefringence

alignment accuracy stability alignment control

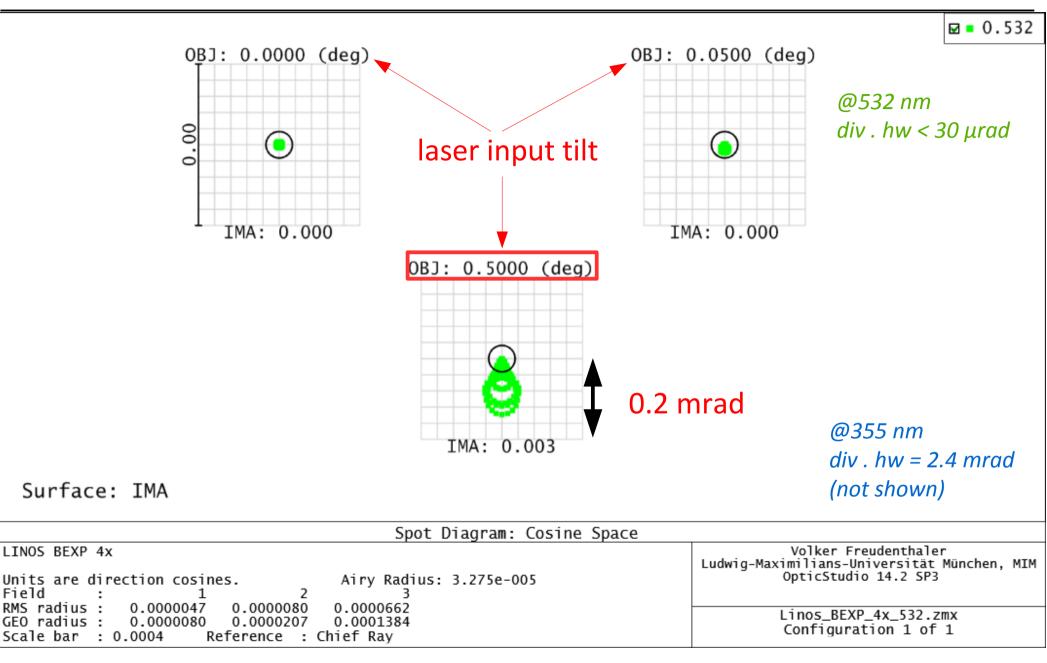
polarisation orientation flatness



Emitter optics – LINOS 4x beam expander simulation (silica lenses)



Emitter optics - LINOS 4x beam expander parallel input => output angle distribution



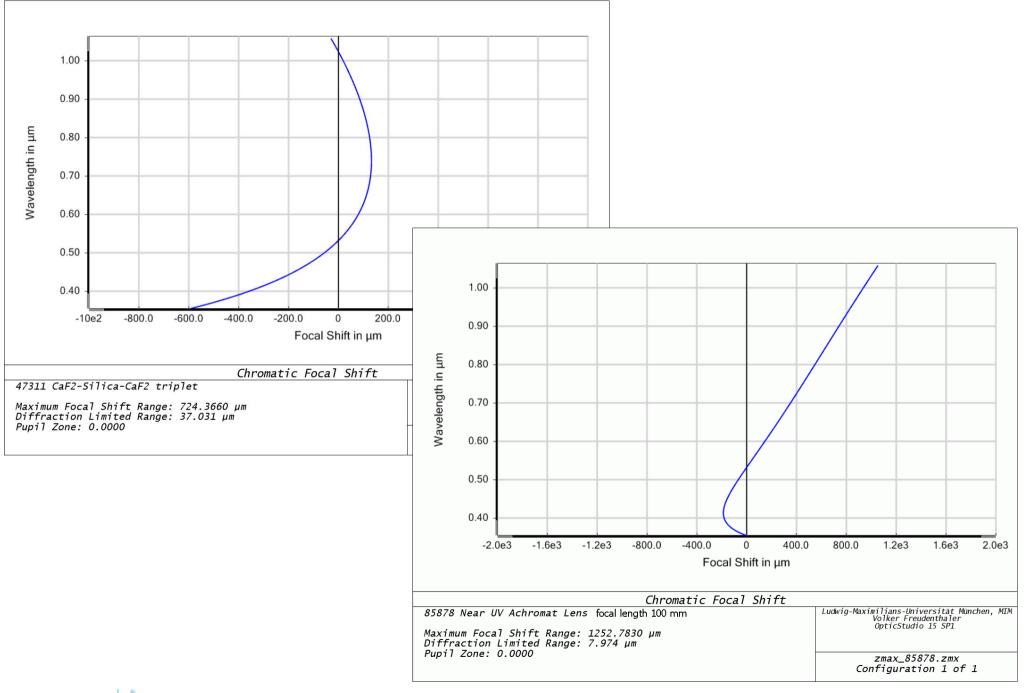
Angular spot diagrams for 0°, 0.05°, and 0.5° tilted input, showing a performance better than the diffraction limit (black circle). At laser input tilt of 0.5° (lower plot) already 0.14 mrad distortions (hw).



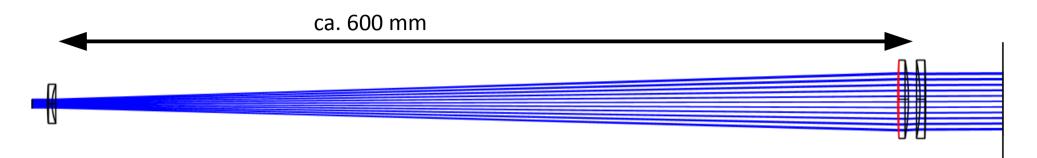
Field.

37

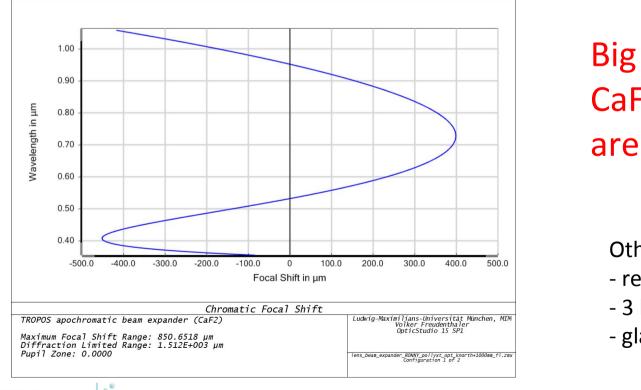
Emitter optics – beam expander with achromats







Engelmann, R., et al., The Automated Multiwavelength Raman, Polarization, and Water-Vapor Lidar Polly XT : The NeXT Generation, AMT, 2016. http://www.atmos-meas-tech.net/9/1767/2016/amt-9-1767-2016.html



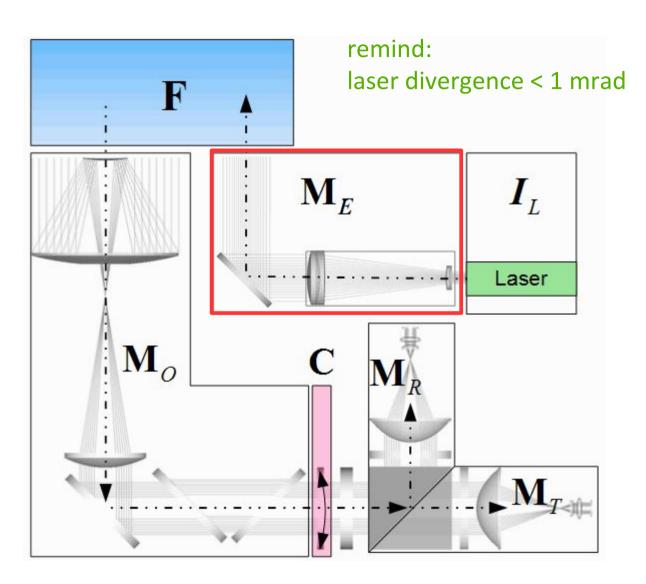
A 🛈 T R i S

Aerosol, Clouds and Trace gases Research InfraStructure

Big problem: CaF2 and MgF2 lenses are birefringent

Other problems:

- residual wavelength dependence
- 3 lambda AR-coating
- glass solarisation



emitter and steering optics

wavelength dependence
focal length => divergence
transmission
polarisation
birefringence

alignment

accuracy stability alignment control

polarisation orientation flatness







remind: laser divergence < 1 mrad

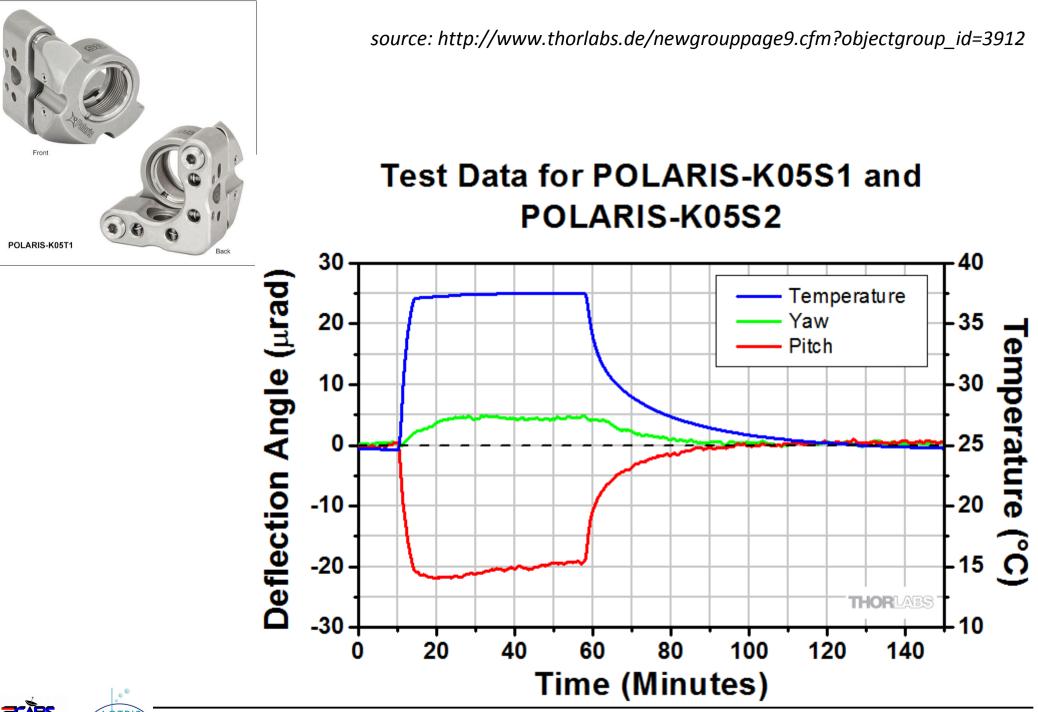
0.5" Resolution: <u>13 mrad</u> (0.75°) per Rev

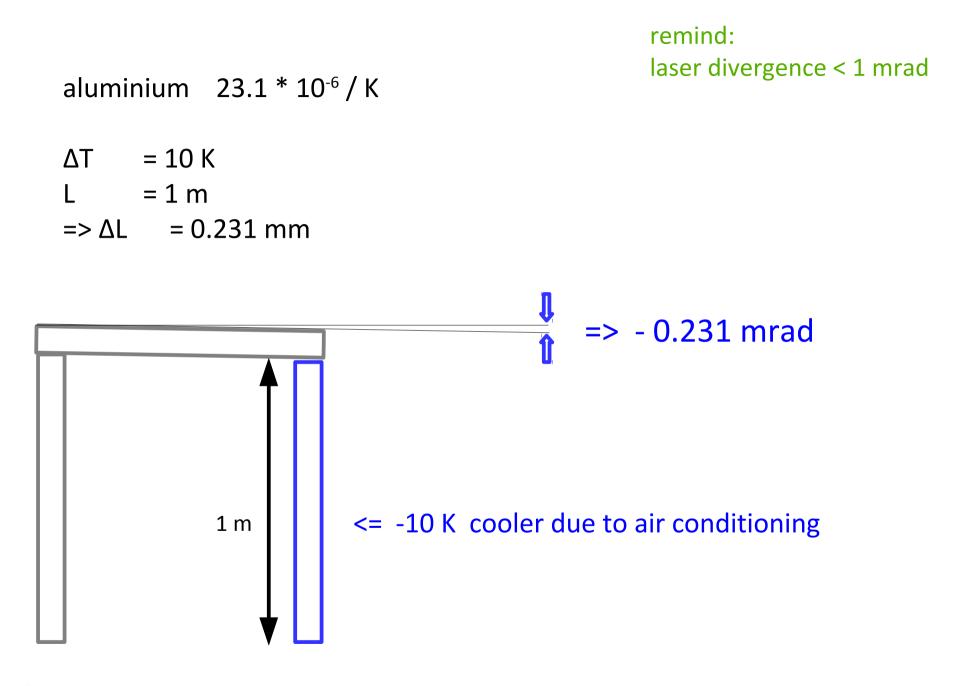
1" Resolution: <u>8 mrad</u> (0.5°) per Rev



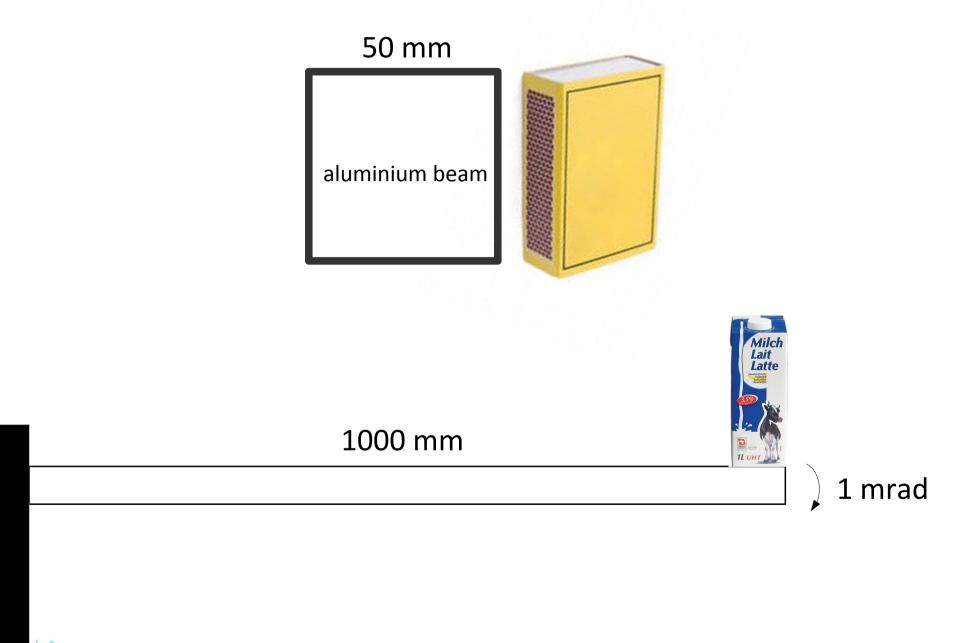
2" Resolution: <u>5 mrad</u> (0.3°) per Rev

EXCEPS The European Centre for Merosole, Clouds and Trace gases Merosole, Clouds and Trace gases source: http://www.thorlabs.de/search/thorsearch.cfm?search=Kinematic%20Mount







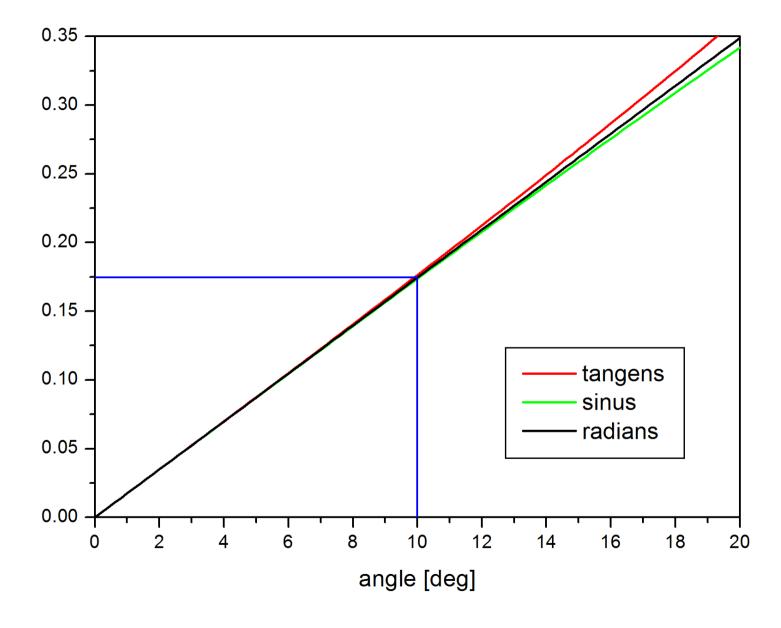




CTRIS

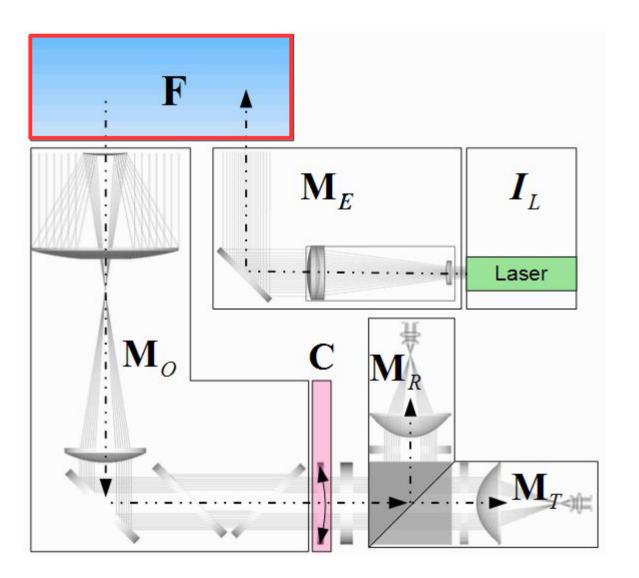
ls and Trace gases rch InfraStructure







46



atmosphere

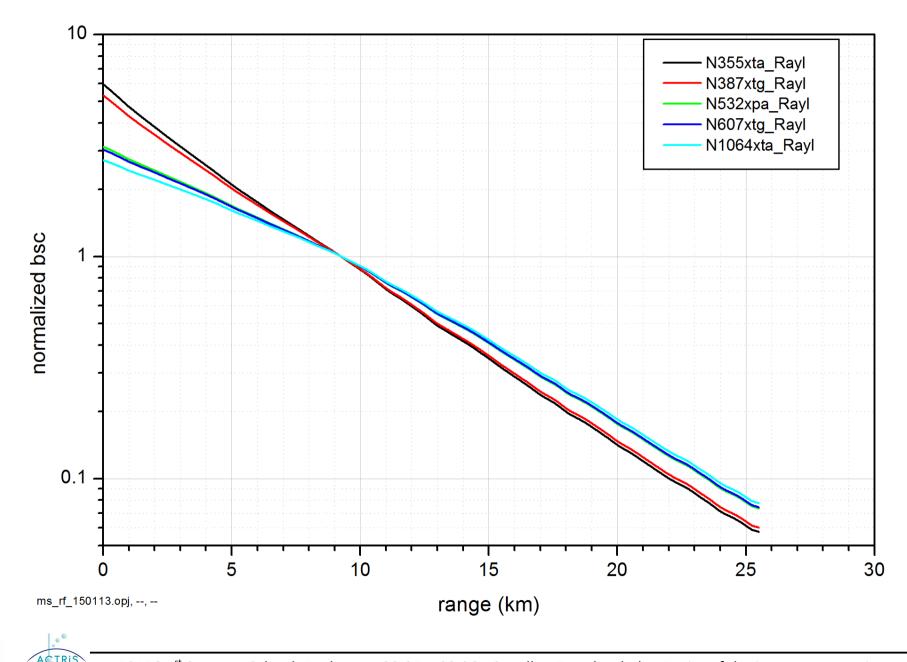
Rayleigh calibration

Rayleigh

backscatter coefficients depolarisation ratios Raman lines in IFF bw

radiosonde data







erosol, Clouds and Trace gas Research InfraStructu Rayleigh scattering (extinction) cross section

$$\sigma_m(z,\lambda) = C_s(\lambda) \frac{p(z)}{T(z)}$$

and backscatter coefficients

for the Cabannes line (^c) and total (⁷) Rayleigh scattering

$$\beta_m^{C,T}(z,\lambda) = B_s^{C,T}(\lambda) \frac{p(z)}{T(z)}$$

from atmospheric pressure p and temperature T depending on height z.

http://www.meteo.physik.uni-muenchen.de/~stlidar/earlinet_asos/Rayleigh_scattering/Rayleigh_coefficients.pdf



Rayleigh calibration: absolute backscatter coefficient and extinction (slope)

wave- length	(n _s - 1)	King factor F _k	C _s	$\mathbf{B}_{\mathbf{s}}^{\mathrm{T}}$	B_{s}^{C}	k _{bw} ^T	k _{bw} C	$\sigma_{\rm m}$	β_m^{T}	β_m^{C}	$\delta_m^{\ T}$	δ_m^C
(air/vacuum)			(17)(14)(10)	(18)	(18)	(20)	(22)	(17)	(18)	(18)	(15)	(16)
[nm]	[*1e-8]		[K/hPa/m]	[K/hPa/ (m*sr)]	[K/hPa/ (m*sr)]			[1/m]	[1/(m*sr)]	[1/(m*sr)]	[*1e-2]	[*1e-2]
	STD air	STD air						STD air	STD air	STD air	STD air	STD air
308 / 308.089	29046.6	1.05574	3.6506e-5	4.2886E-6	4.1678E-6	1.01610	1.04554	1.2837E-4	1.5080E-5	1.4656E-5	0.01636	0.004158
351 / 351.100	28602.7	1.05307	2.0934e-5	2.4610E-6	2.3949E-6	1.01535	1.04338	7.3611E-5	8.6539E-6	8.4214E-6	0.01559	0.003959
354.717 / 354.818	28572.4	1.05290	2.0024E-5	2.3542E-6	2.2912E-6	1.01530	1.04324	7.0414E-5	8.2783E-6	8.0566E-6	0.01554	0.003946
355 / 355.101	28570.2	1.05288	1.9957E-5	2.3463E-6	2.2835E-6	1.01530	1.04323	7.0177E-5	8.2506E-6	8.0393E-6	0.01554	0.003946
<u>386.890 / 387.000</u>	28350.2	1.05166	1.3942e-5					4.8925E-5				
400 / 400.113	28275.2	1.05125	1.2109E-5	1.4242E-6	1.3872E-6	1.01484	1.04191	4.2579E-5	5.00810E-6	4.8780E-6	0.01507	0.003825
<u>407.558 / 407.673</u>	28235.1	1.05105	1.1202e-5					3.9389E-5				
510.6 / 510.742	27869.4	1.04922	4.4221E-6	5.2042E-7	5.0742E-7	1.01427	1.04026	1.5550E-5	1.8300E-6	1.7843E-6	0.01448	0.003673
532 / 532.148	27819.9	1.04899	3.7382E-6	4.3997E-7	4.2903E-7	1.01421	1.04007	1.3145E-5	1.5471E-6	1.5086E-6	0.01441	0.003656
532.075 / 532.223	27819.4	1.04899	3.7361E-6	4.3971E-7	4.2878E-7	1.01421	1.04007	1.3138E-5	1.5462E-6	1.5078E-6	0.01441	0.003656
<u>607.435 / 607.603</u>	27686.3	1.04839	2.1772e-6					7.6559E-6				
710 / 710.196	27570.4	1.04790	1.1561E-6	1.3611E-7	1.3280E-7	1.01390	1.03919	4.0655E-6	4.7863E-7	4.66698E-7	0.01410	0.003575
800 / 800.220	27503.8	1.04763	7.1364E-7	8.4022E-8	8.1989E-8	1.01383	1.03897	2.5094E-6	2.9546E-7	2.8831E-7	0.01402	0.003555
1064 / 1064.292	27397.5	1.04721	2.2622E-7	2.6638E-8	2.5999E-8	1.01371	1.03863	7.95949E-7	9.3670E-8	9.1423E-8	0.01390	0.003524
1064.150 / 1064.442	27397.4	1.04721	2.2609E-7	2.6623E-8	2.5984E-8	1.01371	1.03863	7.9504E-7	9.3617E-8	9.1371E-8	0.01390	0.003524

Table of scattering conversion factors and related values (ver. 1.4f)

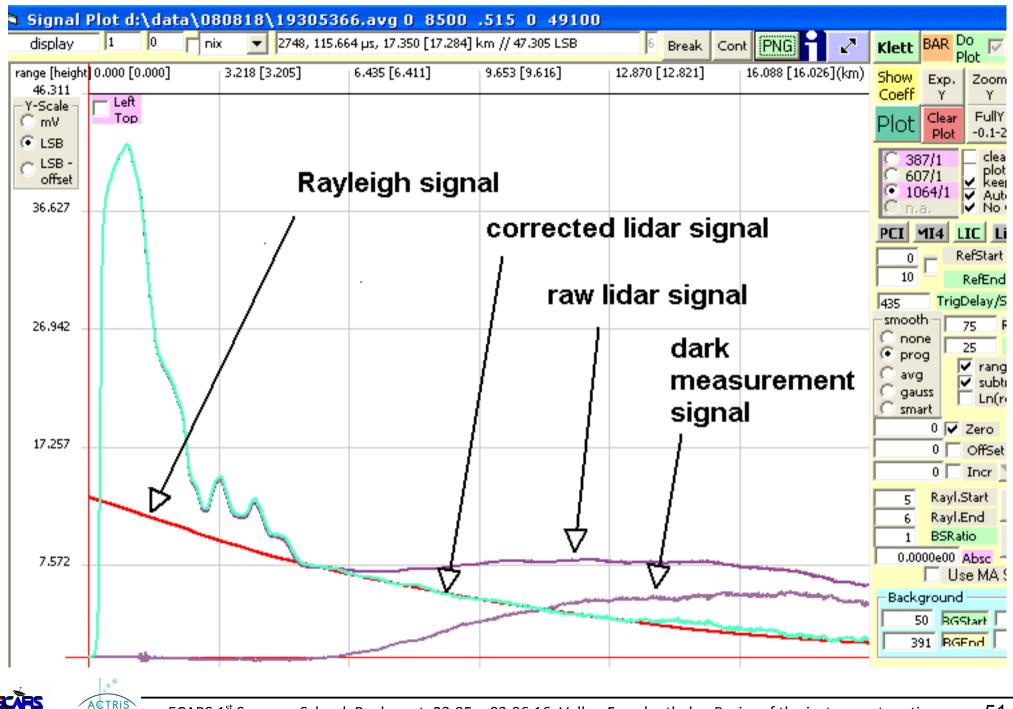
Table 1: Refractive index (n_s) , King factor (F_k) , extinction coefficients (σ_m) , Cabannes (β_m^C) and total Rayleigh (β_m^T) backscatter coefficients, proportionality factors (see text above), and Cabannes (δ_m^C) and total Rayleigh (δ_m^T) linear depolarisation ratios caclulated with the equations in row two, for STD air conditions where mentioned (STD air: $p_s = 1013.25$ hPa, $T_s = 288.15$ K). The refractive indices and the King factors are calculated according to Tomasi et al. (2005) and Ciddor (2002) with 385 ppmv CO₂ and 0% RH. Please note that the values in the table of the Tomasi paper were caclulated for slightly different conditions. NdYAG elastic and Raman wavelenghts (underlined) are for vacuum, calculated from the fundamental air wavelength 1064.15 nm (1064.442 nm in vacuum) at 300 K rod temperature according to Kaminskii. (RAMAN3G.ods, Laserlinien.ods, Rayleigh1.vbs) (This table is version 1.4f from Feb. 2013: some "exact" wavelengths added to version 1.1 and corrected from ver. 1.3; 1.4f: wavelengths in air and vacuum). In order to enable the comparison of the accuracy of the calculatuions by the readers, more decimal digits are shown than certified by the accuracy of the model and the assumtions.

http://www.meteo.physik.uni-muenchen.de/~stlidar/earlinet_asos/Rayleigh_scattering/Rayleigh_coefficients.pdf

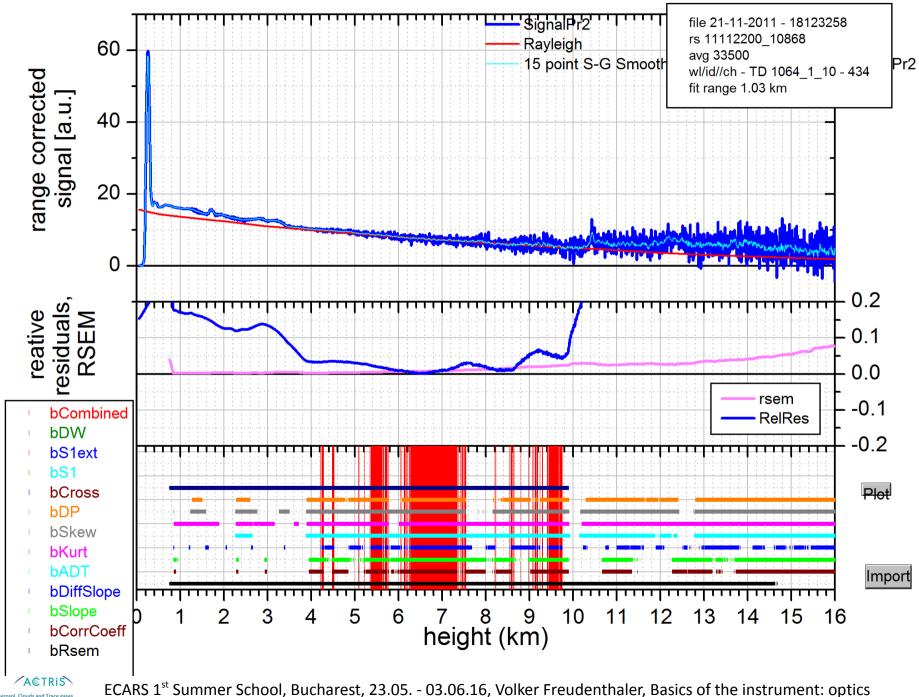
ast European Centre for Aerosol, Clouds and Tr

ECARS 1st Summer School, Bucharest, 23.05. - 03.06.16, Volker Freudenthaler, Basics of the instrument: optics

Rayleigh calibration: absolute backscatter coefficient and extinction (slope)

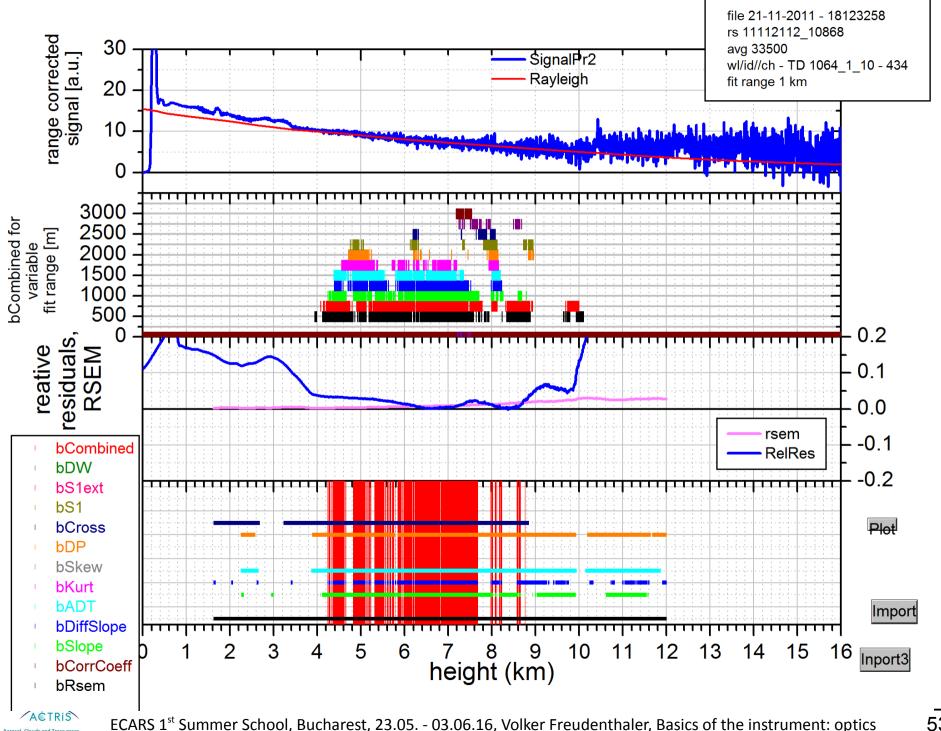


Aerosol, Clouds and Trace gases Research InfraStructure



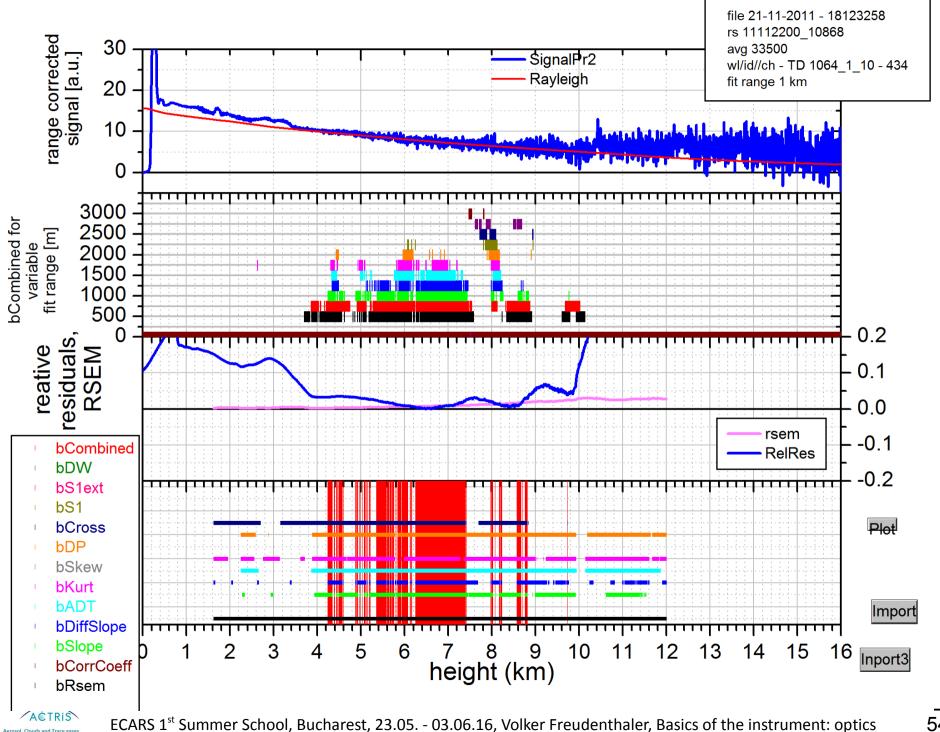
Rayleigh calibration: quality checks

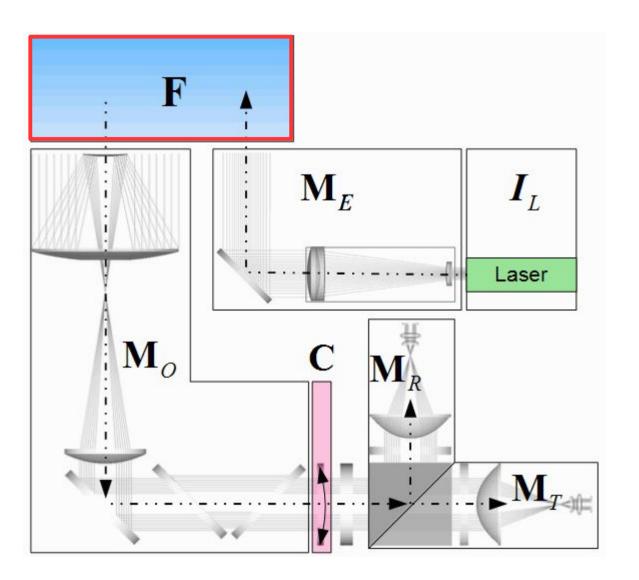
Aerosol, Clouds and Trace gases Research InfraStructure



Rayleigh calibration: quality checks

Aerosol, Clouds and Trace gases Research InfraStructure





atmosphere

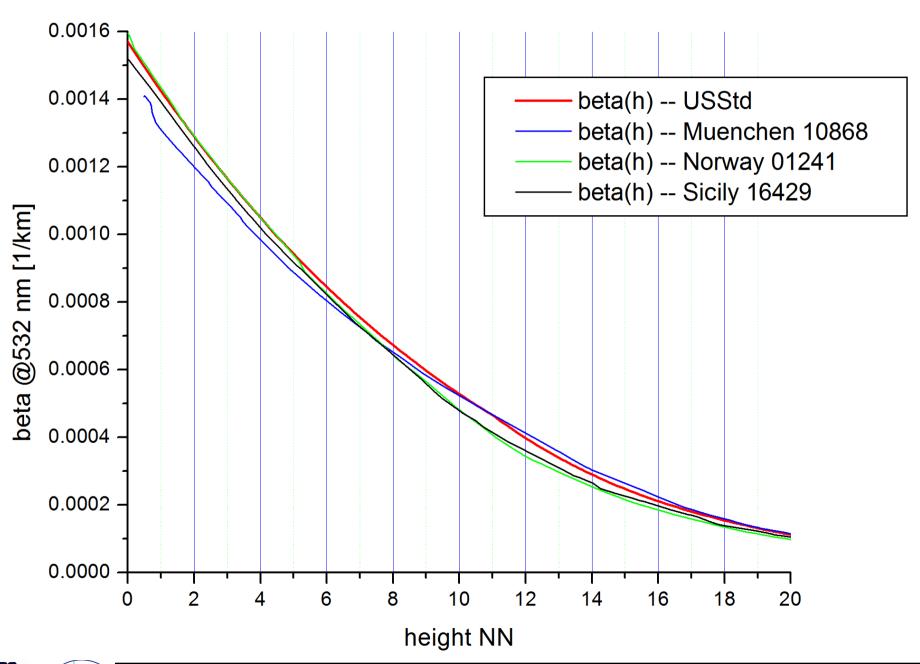
Rayleigh calibration

Rayleigh

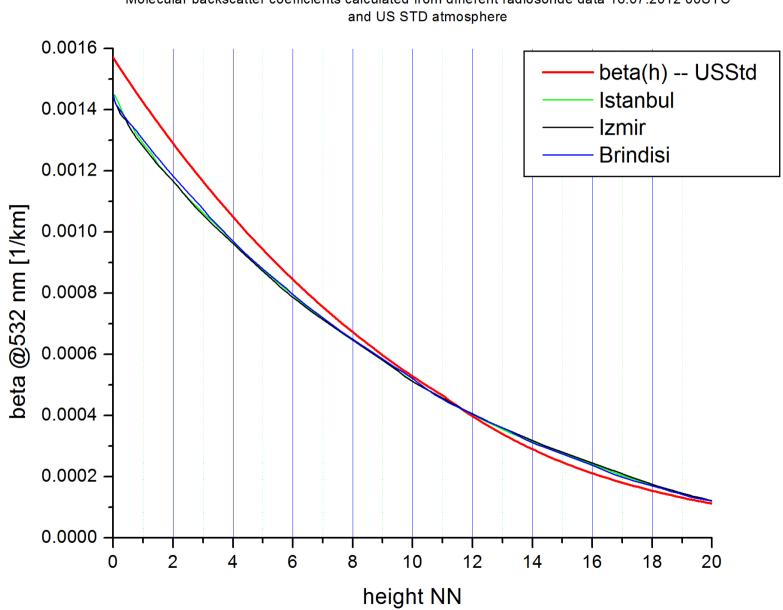
backscatter coefficients depolarisation ratios Raman lines in IFF bw

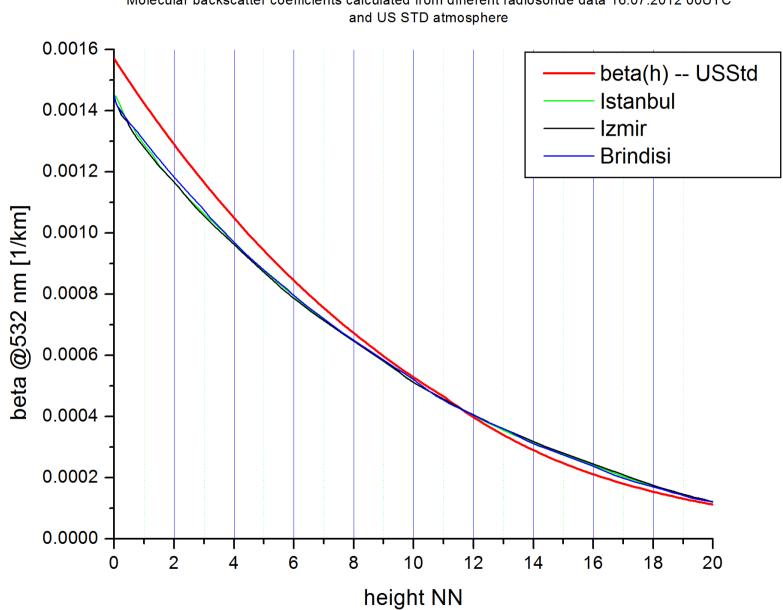
radiosonde data





Molecular backscatter coefficients calculated from different radiosonde data and US STD atmosphere





Radiosonde data:

http://weather.uwyo.edu/upperair/sounding.html

Modell data:

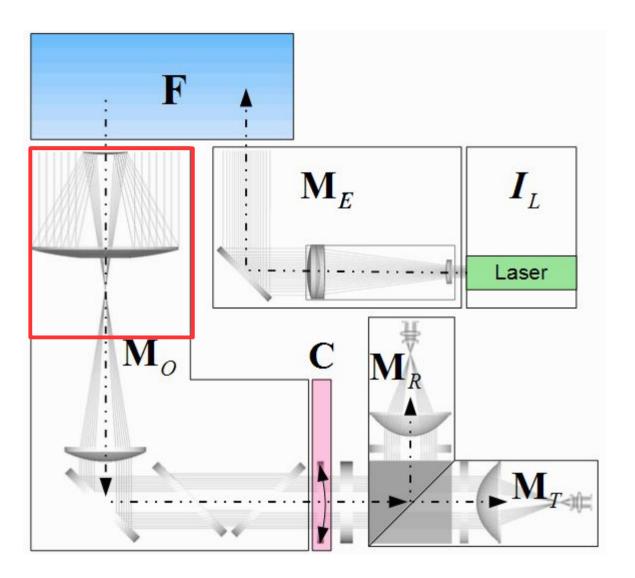
http://rucsoundings.noaa.gov/

EARLINET forum: earlinetforum.imaa.cnr.it => topic: QA Rayleigh-fit and radiosonde

http://www.meteo.physik.uni-muenchen.de/~stlidar/earlinet_asos/Rayleigh_scattering/EA-radiosondes.html

- => Generate soundings from model analysis and forecast
- => Generate soundings from archived model data
- => Archived soundings from radio sondes





receiving optics telescope

focal length, diameter

alignment stability

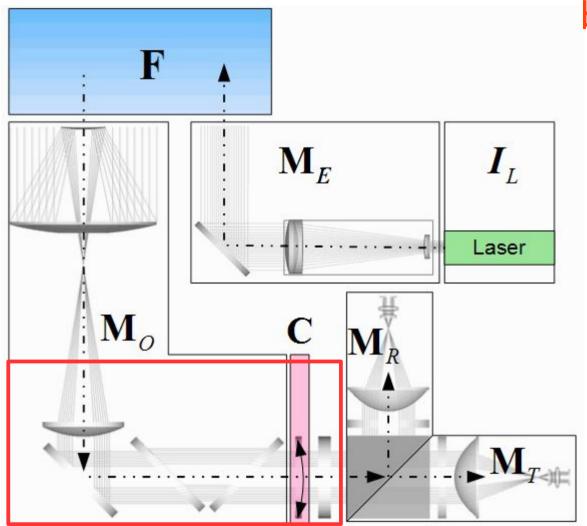
Newton telescope 90° mirror depolarisation

field of view

distance of full overlap

60





receiving optics beamsplitters and filters

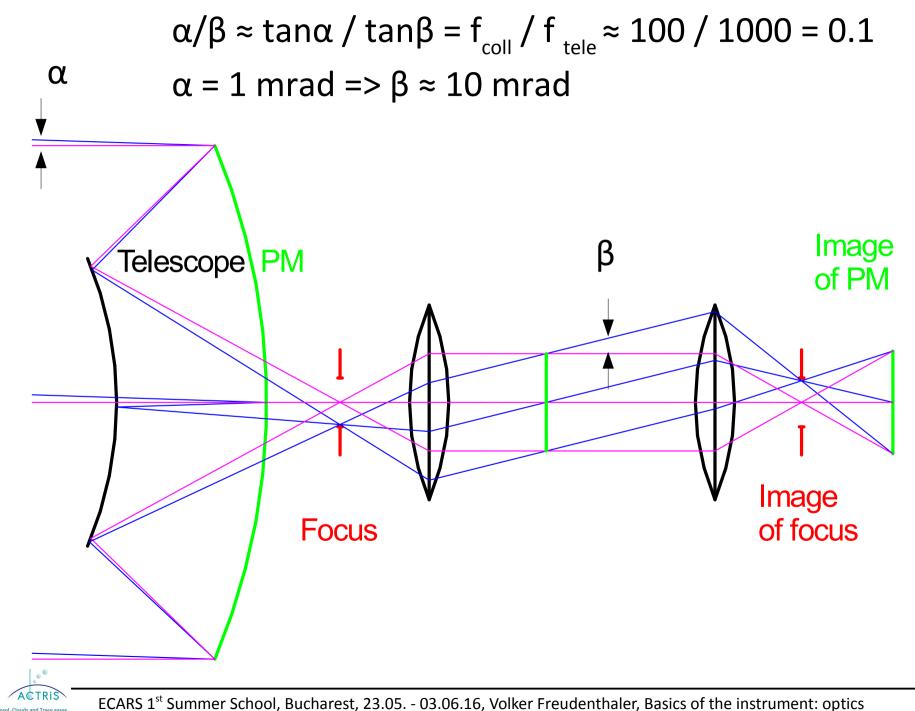
focal length of collimator => optics beam divergence => optics beam diameter

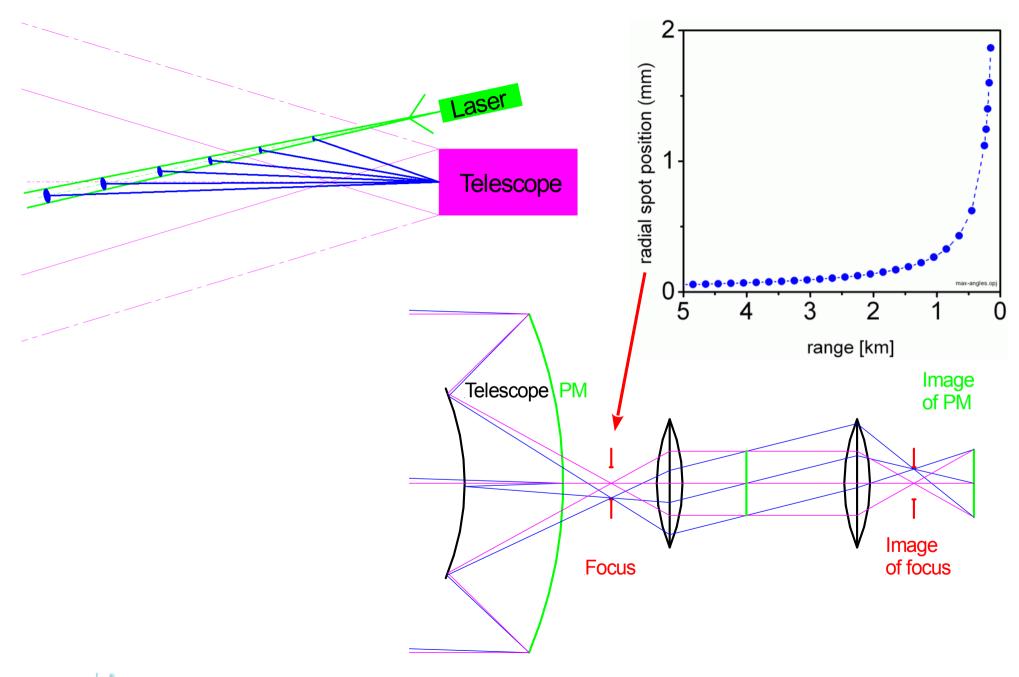
accpetance angles of beamsplitters and interference filters

polarisation problemes diattenuation retardance

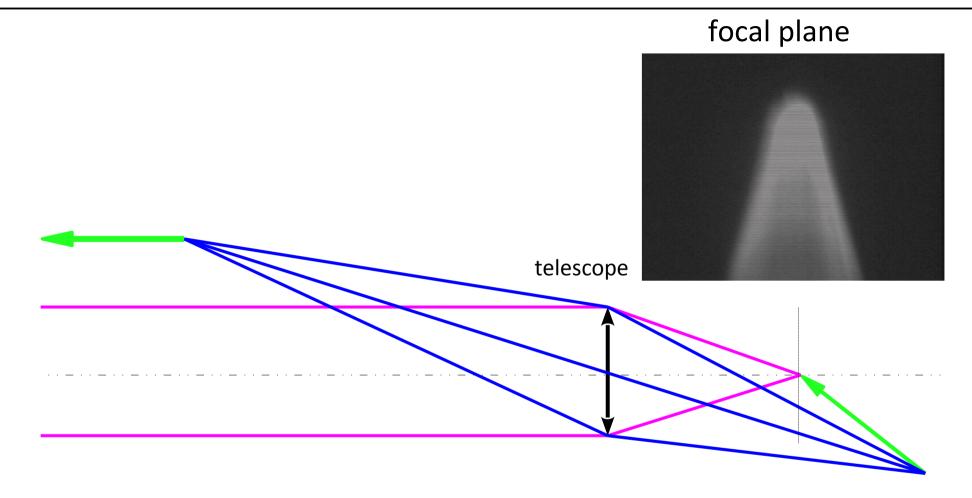


Research InfraStructu





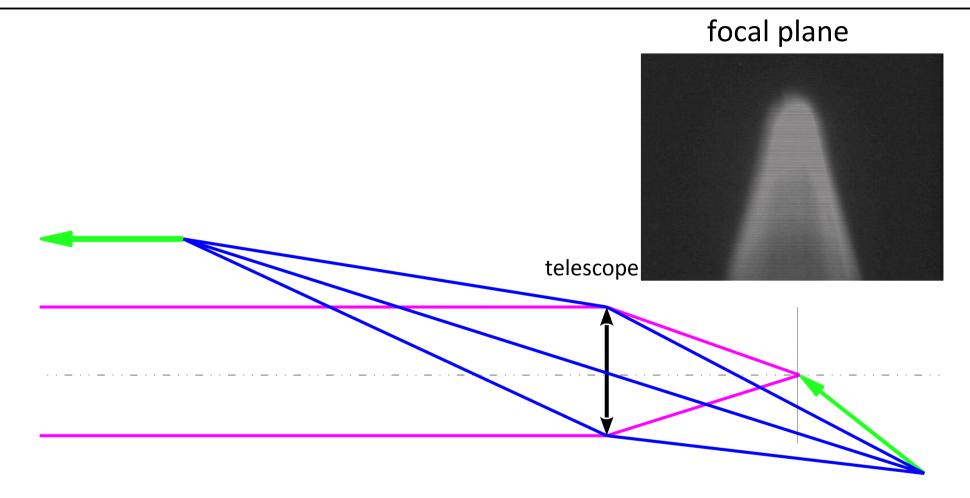




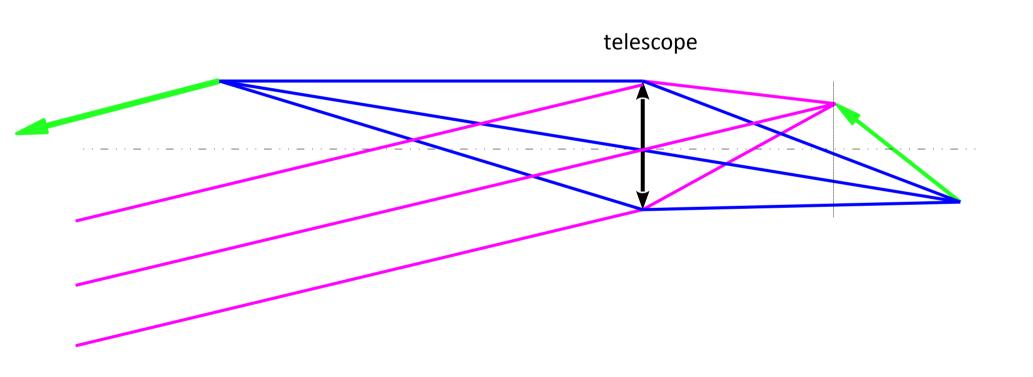


behind focal plane telescope



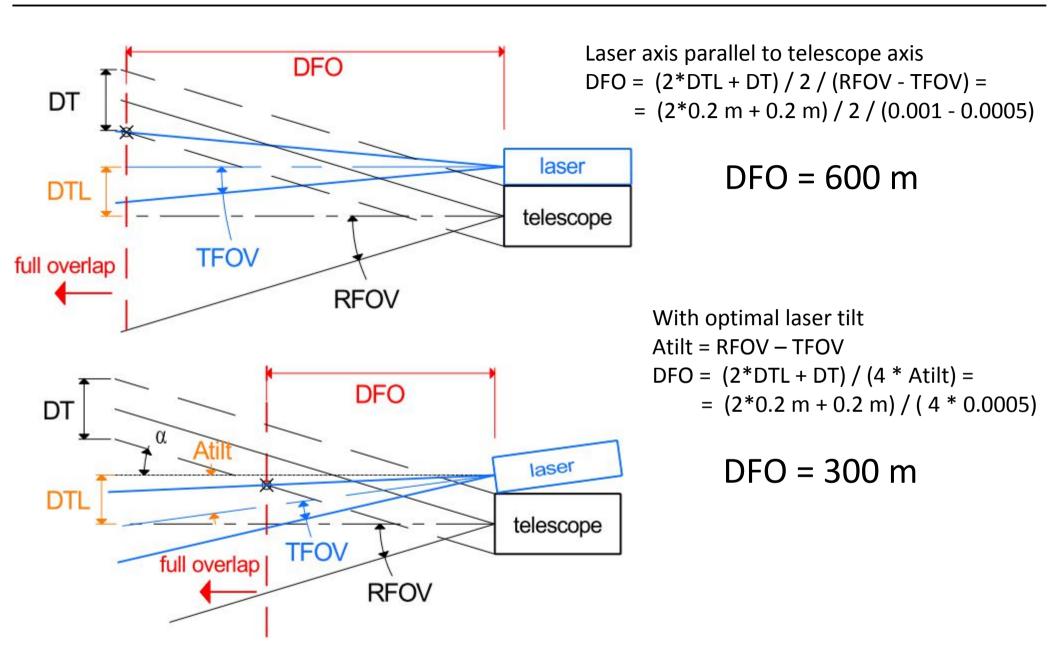








68



V. Freudenthaler, "Optimized background suppression in near field lidar telescopes", 6th ISTP Int. Symposium on Tropospheric Profiling, 14. - 20. Sept. 2003, Leipzig, Germany, (2003). URN urn:nbn:de:bvb:19-epub-12957-5, available online: http://epub.ub.uni-muenchen.de/12957/



Explanations:

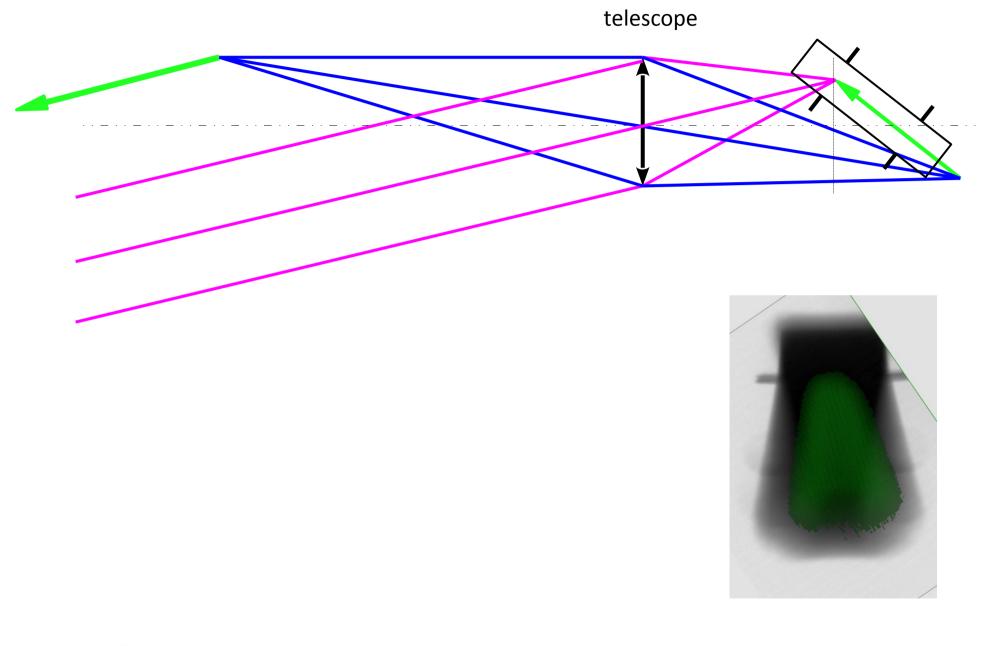
www.meteo.physik.uni-muenchen.de/~stlidar/earlinet_asos/raytracing/Basic_design/basic_lidar_design.html

EXCEL spreadsheet (basic_lidar_design_ver_1.0.xls, Panos Kokkalis)

www.meteo.physik.uni-muenchen.de/~stlidar/earlinet_asos/raytracing/Basic_design/basic_lidar_design_ver_1.0.xls

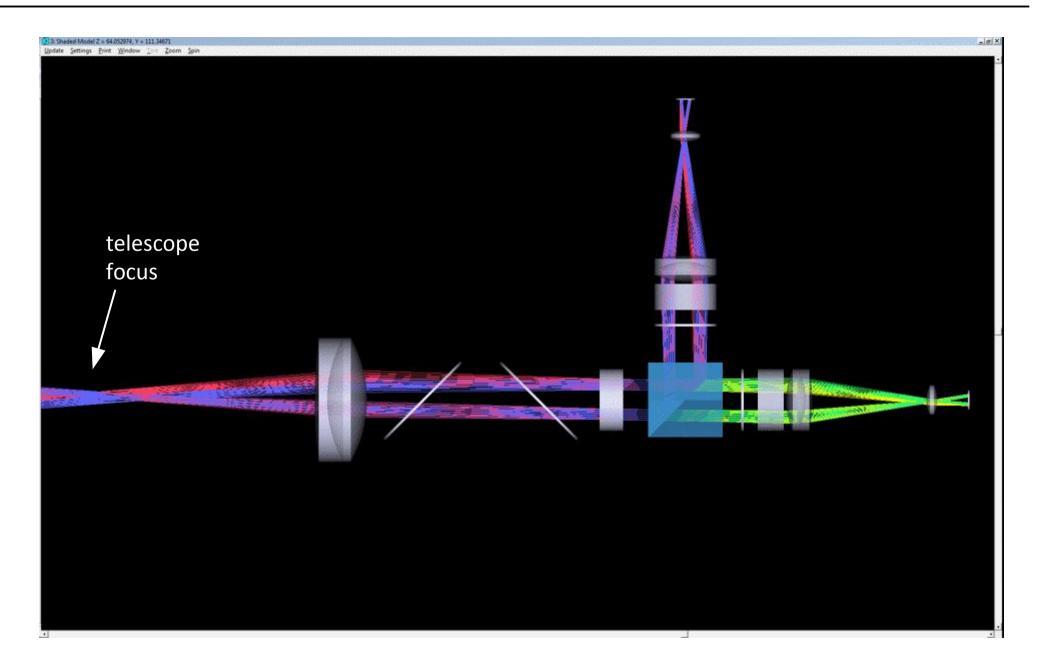
INPUTS		OUTPUTS					
Laser		Depending only on laser and telescope					
Atilt (mrad)	0.50	Atilt max (mrad)	0.560				
TFOV nominal (mrad)	0.60	DFOmin (m) @ Atilt max	405.36				
Dlaser (mm)	8.00	DFO (m)	428.30				
GaussSizeFactor	3.00						
Beam Expander x	1.00						
TFOV expanded (mrad)	0.900						
Dlaser expanded (mm)	8.00						
Telescope		CURRENT SYSTEM					
DTL (mm)	300.00	FCOL (mm)	50.00				
FT (mm)	1200.00	DCOL (mm)	16.15				
DT (mm)	300.00	A (deg)	2.008				
DFieldstop (mm)	3.00	ZII (mm)	52.08				
RFOV (mrad)	1.50	DII (mm)	12.50				
RFOV tolerance (mrad)	0.04	Z1 (mm)	444.49				
effective RFOV (mrad)	1.460	ZOBJ (mm)	392.41				
Behind the Diaphragm (FOVD)		DOBJ (mm)	40.000				
FCOL (mm)	50.000	FOBJ (mm)	80.00				
		FEYE (mm)	32.00				
DOBJ (mm)	40.000	DEYE (mm)	1.849				
FOBJ / DOBJ	2.00	Z2 (mm)	112.00				
DPMT (mm)	5.00	Z3 (mm)	-17.985				



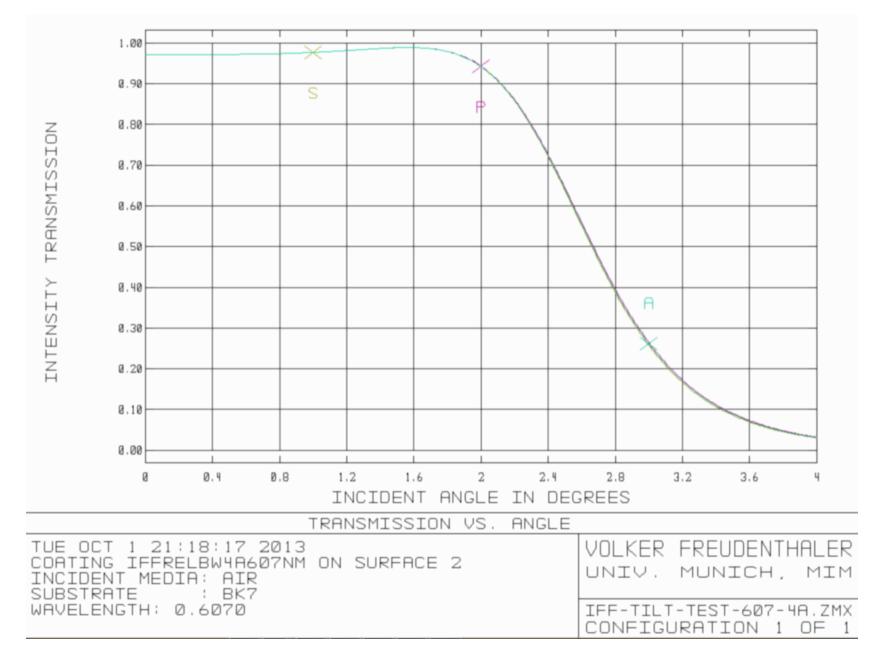




Spatial and angular beam truncation by apertures and coatings







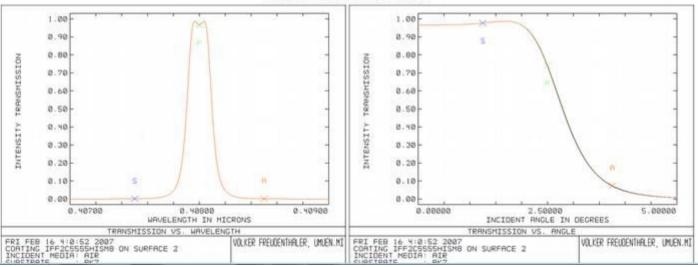


Introduction, explanations, database

www.meteo.physik.uni-muenchen.de/~stlidar/earlinet_asos/raytracing/IFF/EA-IFFilters.html

Centre wl [nm]	355	BW	neff	2	387	BW	neff	φ	400	408	BW	neff	φ	511	532	BW	neff	q
IFF BW (nm)																		
0.14															IFF2C5555SCLISM2	0.14	1.48	1
															IFF2C4444SCHISM4	0.14	2.04	1
0.2	FF2C5555HISM3	0.22	2.01	2.5	IFF2C5555HISM5	0.22	1.97	2.45		IFF2C5555HISM8	0.2	2	2.2		IFF2C5555HISM20	0.19	2.01	à
	FF2C4444HISM10	0.2	2.17	2.7											IFF2C5555HISM22	0.18	2.01	
															IFF2C4444SCHISM3	0.18	1.99	
0.3	FF2C4444HISM6	0.31	2.1	3.2														
0.35									1						1			
0.42										1					A CONTRACTOR OF A DESCRIPTION			
0.5	FF2C3333HISM9	0.52	2.12	4.2	IFF2C4444HISM5	0.48	1.97	3.7		IFF2C4444HISM7	0.48	1.99	3.4	1	IFF2C4444HISM15	0.5	1.99	
										IFF2C3333HISM16	0.52	2.05	3.7					
1	FF2C3333HISM4	0.98	2.05	6.8						IFF2C3333HISM8	0.94	2	4.8		IFF2C3333HISM16	0.99	1.99	
1.5											_				1			
3	1				1					1					IFF2C2222HISM10	3.0	1.96	

Centre wl [nm]	607	BW nef	fφ	660	710	800	1064	BW	neff	φ
IFF BW (nm)										
0.14										
									_	_

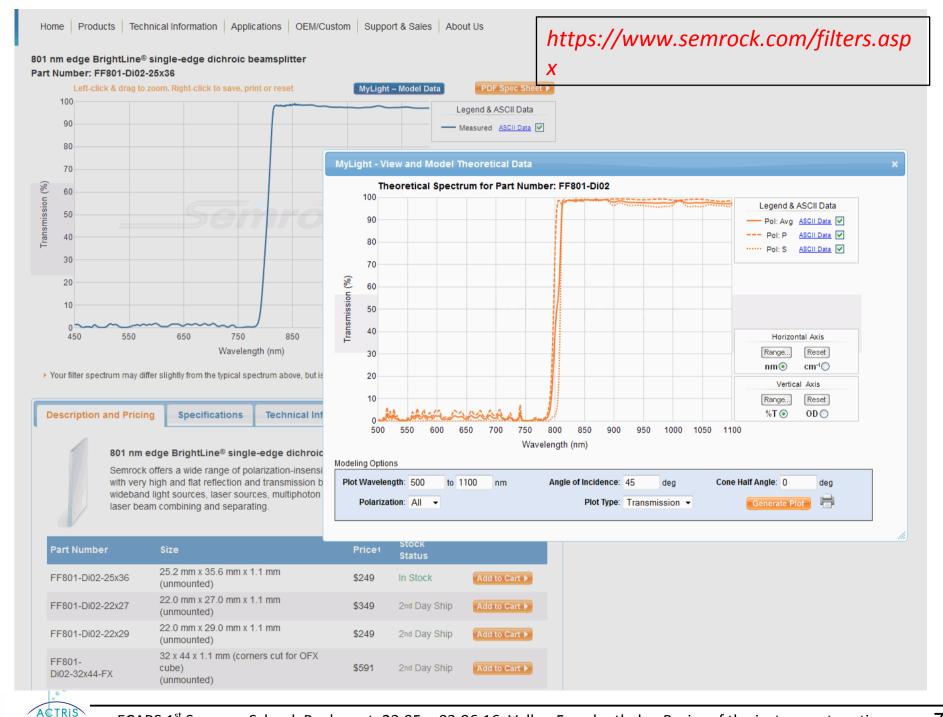


408-IFF2C5555HISM8

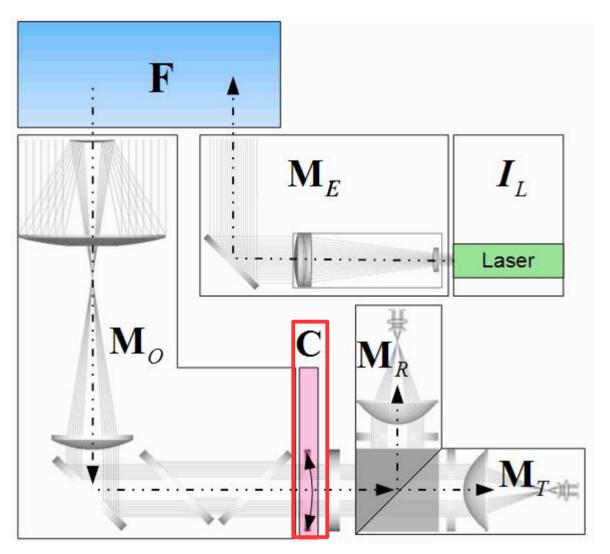
East European Centre for Atmospheric Remote Sensing Research InfraStructure

ECARS 1st Summer School, Bucharest, 23.05. - 03.06.16, Volker Freudenthaler, Basics of the instrument: optics

SEMROCK filter simulator



st European Centre for mospheric Remote Sensing Research InfraStructure



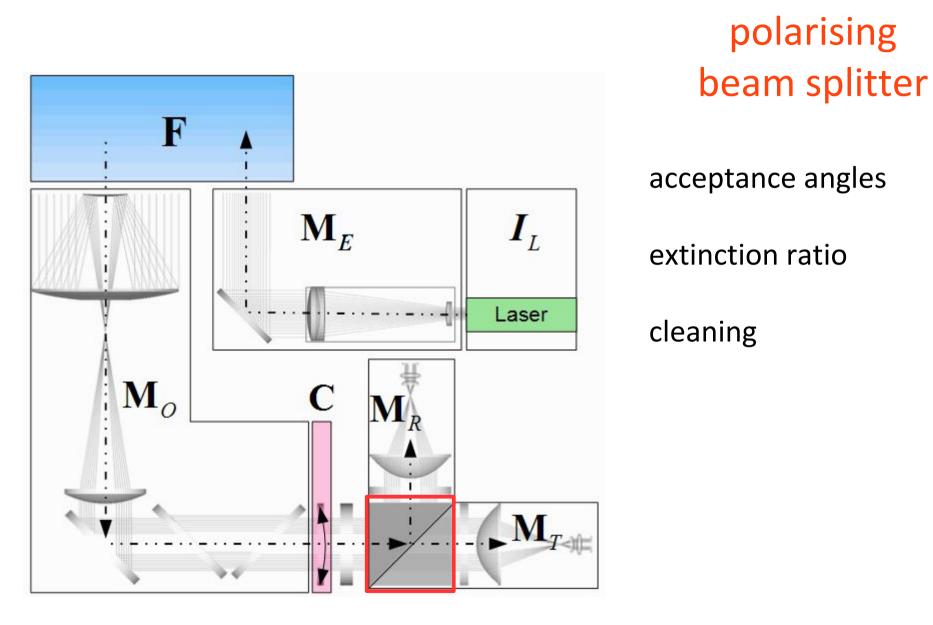
polarisation calibrator

location

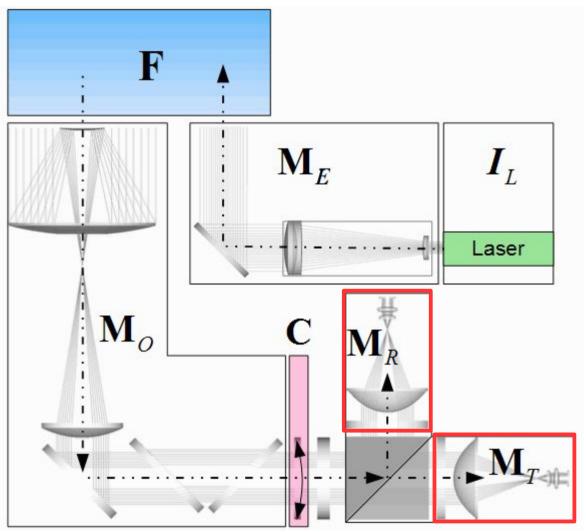
type

parameters to determine









detectors and optics

PMT

homogeneity of the sensitivity

APD

small diameter

eyepiece

=> telescope imaging

neutral density filters
=> adjust signal level (LICEL)

78





assembled in many Hamamatsu photosensor and photocounting modules like



very small size =>
fastest rise time =>
highest count rate and dynamic range
+ relatively insensitive to magnetic fields
used also in LICEL lidar data aquisition



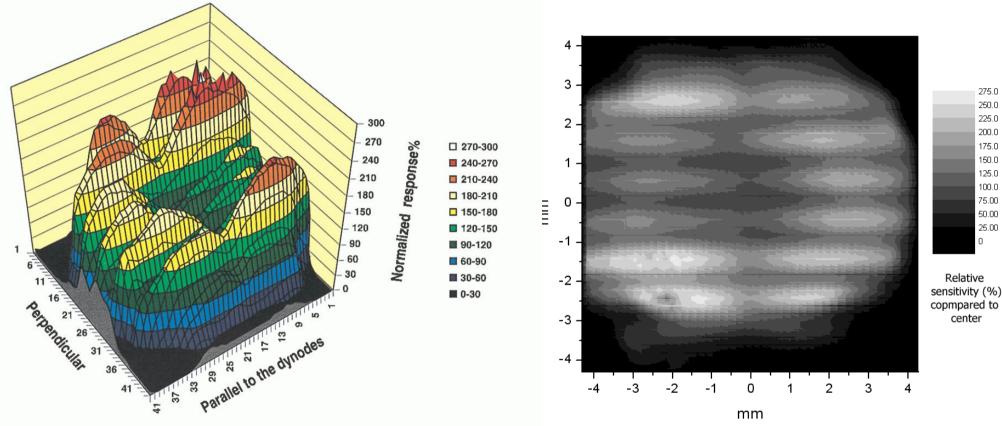
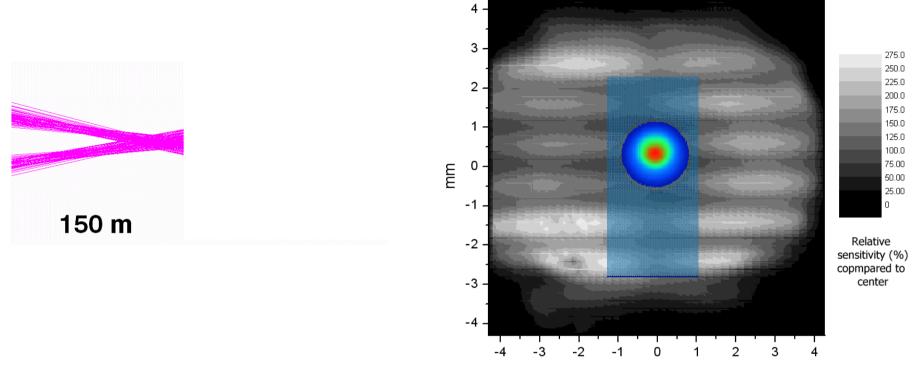


Fig. 1. Anode spatial uniformity of the Hamamatsu H5783-06 photosensor module measured with a resolution of 200 μ m. The values were normalized to the average of the central part of the photocathode (2 × 2 mm).

source: V. Simeonov et al., Influence of the Photomultiplier Tube Spatial Uniformity on Lidar Signals, Appl. Opt. 38, 5186-5190 August 1999.

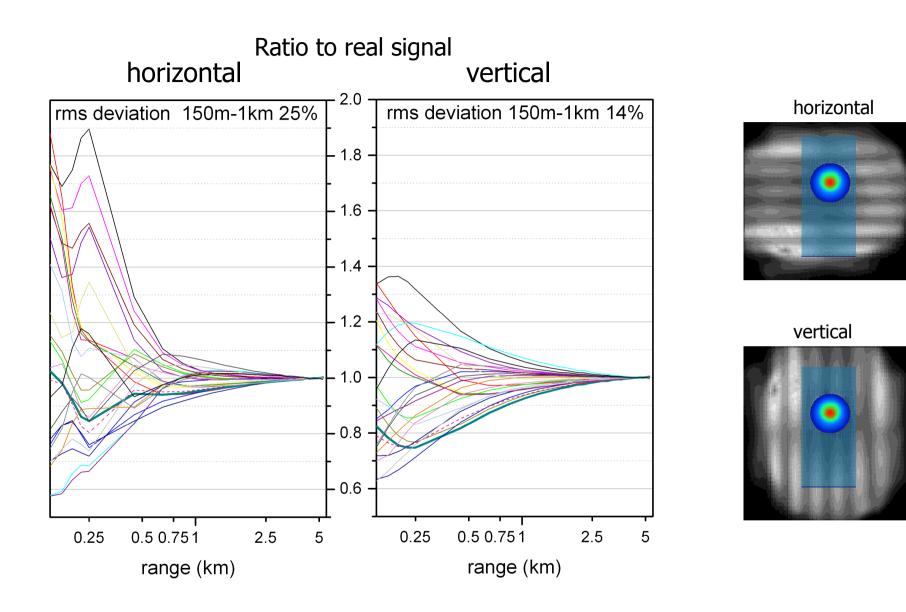




mm

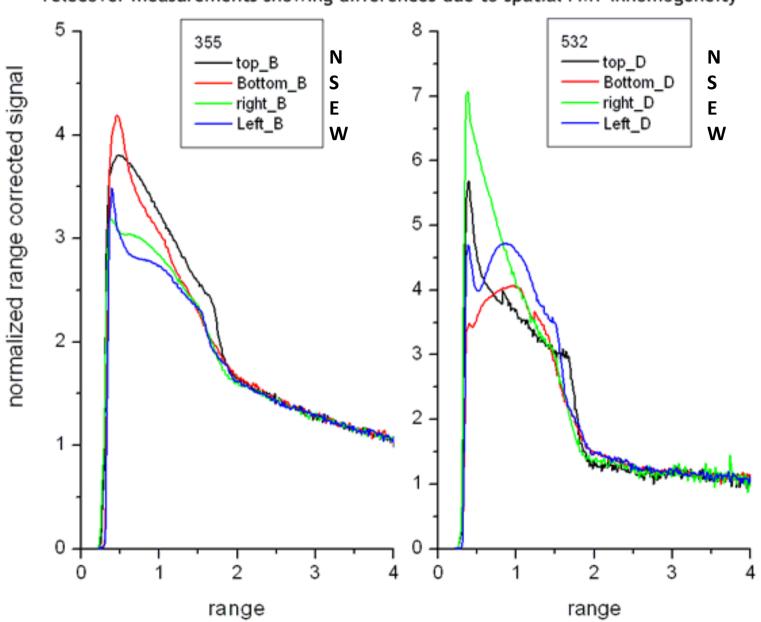
source: V. Freudenthaler, Effects of spatially inhomogeneous photomultiplier sensitivity on lidar signals and remedies, ILRC22, 2004 http://www.meteo.physik.uni-muenchen.de/~st212fre/ILRC22/index.html



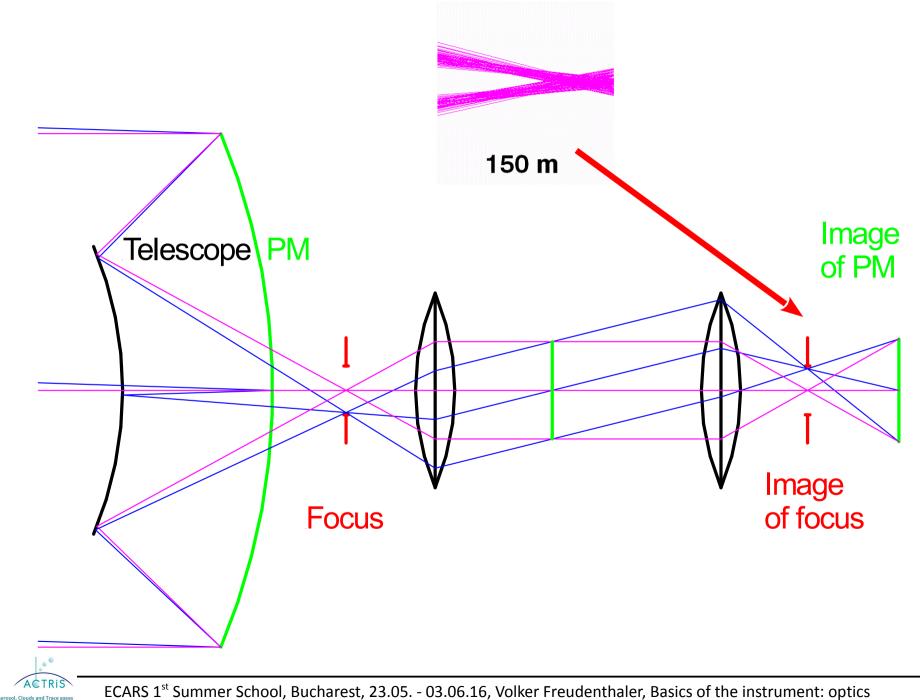


source: V. Freudenthaler, Effects of spatially inhomogeneous photomultiplier sensitivity on lidar signals and remedies, ILRC22, 2004 http://www.meteo.physik.uni-muenchen.de/~st212fre/ILRC22/index.html

East European Centre for Atmospheric Remote Sensing

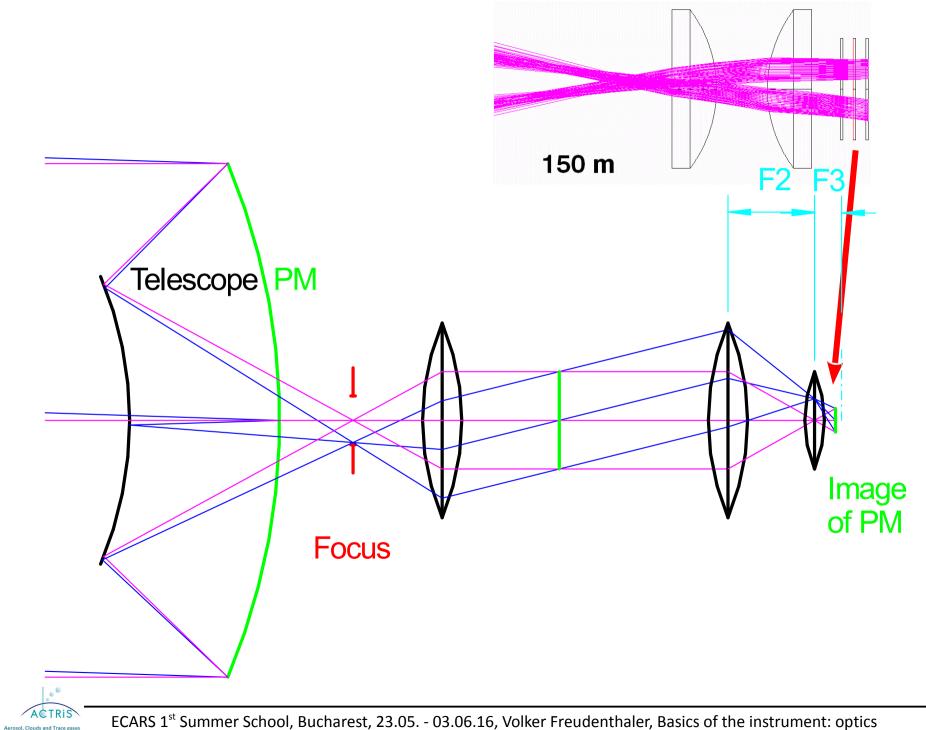


Telecover measurements showing differences due to spatial PMT inhomogeneity

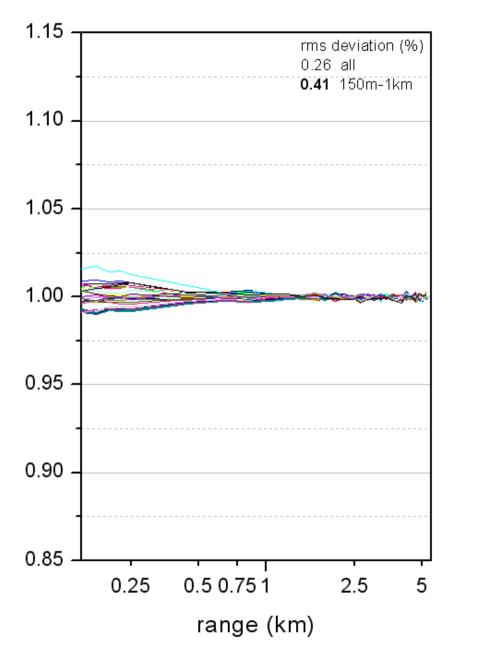


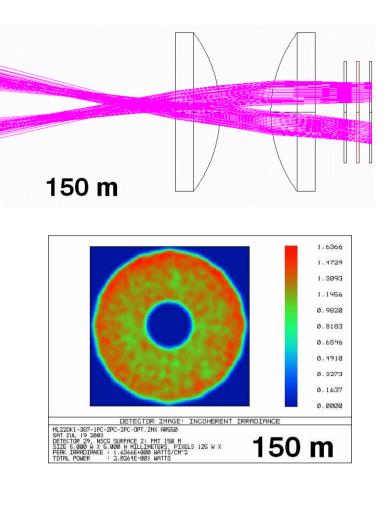
Research InfraStructure

Transmission function, primary mirror image on detector - change with lidar range



Aerosol, Clouds and Trace gases Research InfraStructure

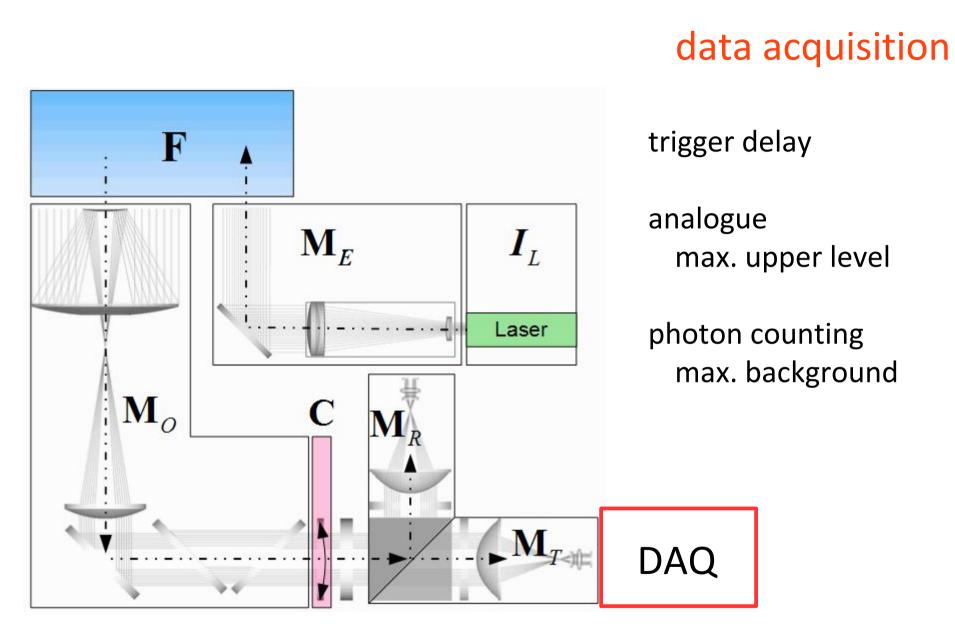




+ Spot does <u>not</u> move
- change of intensity distribution

source: V. Freudenthaler, Effects of spatially inhomogeneous photomultiplier sensitivity on lidar signals and remedies, ILRC22, 2004 http://www.meteo.physik.uni-muenchen.de/~st212fre/ILRC22/index.html



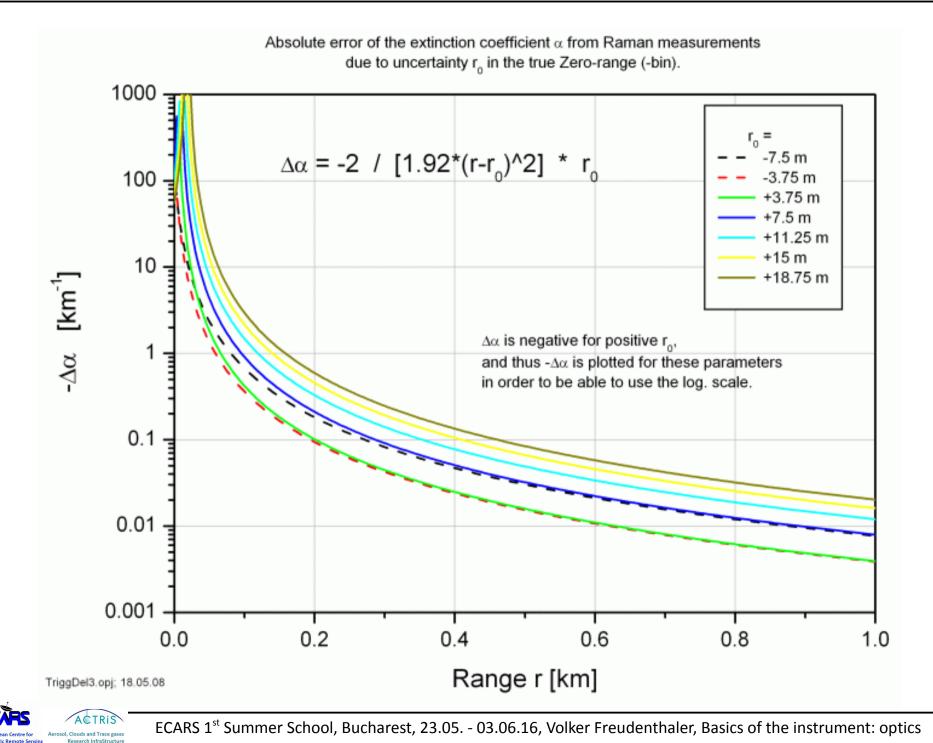




Trigger delay

treigger delay +-2 rangebins = +-15 m Text1 1.97, 3.4637e0 2 P Left -0.134 kn 0 0.495 km 1.124 km abel-x 5.25 1.754 km	Plot1 Plot Eall X
Left -0.134 kn 0 0.495 km 1.124 km abel-x 5.25 1.754 km	Eull X
[1/km]	Plot Clear Zoom Y ExpX
[1/km] 3.215e0	Exc Smooth Dep A Keep plot Err E AutoRedraw 25 RSmo DontCls
0.5208	AlphaA <u>SAVE MA setup</u> GET MA setup
2.361e0	5 WriteStart Save 6 WriteEnd Ncdf
	Text1 OD Start Text2 OD End OD OD SA act.
1.508e0	Text1 ODDiff 0 Text1 ODD% Save Profs Text1 Diff% Text1 Diffabs% Text1 RMS%
6.539e-1	2 LRStart 5 LREnd 2 KonfStart 5 KonfEnd 1 Sincr 0 SSmoo
-1.997e-1	Check 1 MA Pause t Klett DepA
Te THighElev high THref1 THref2 THbsc 🗗 📻 📥	Z 0D1 21
Te TMidElev mid elevation TMref1 TMref2 TMbsc p G Use	
	Calc BSC Z OD3 21 Calc BSC Z OD4 21
Te TLLElev lowest elev TLLref1 TLLref2 TLLbsc P r. Use	

East European Centre for Atmospheric Remote Sensing Research InfraStructure



Trigger delay measurement

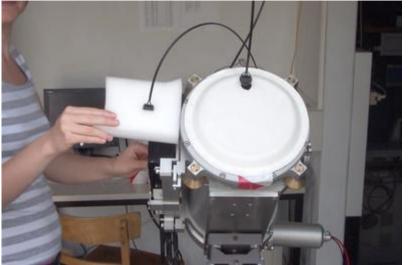








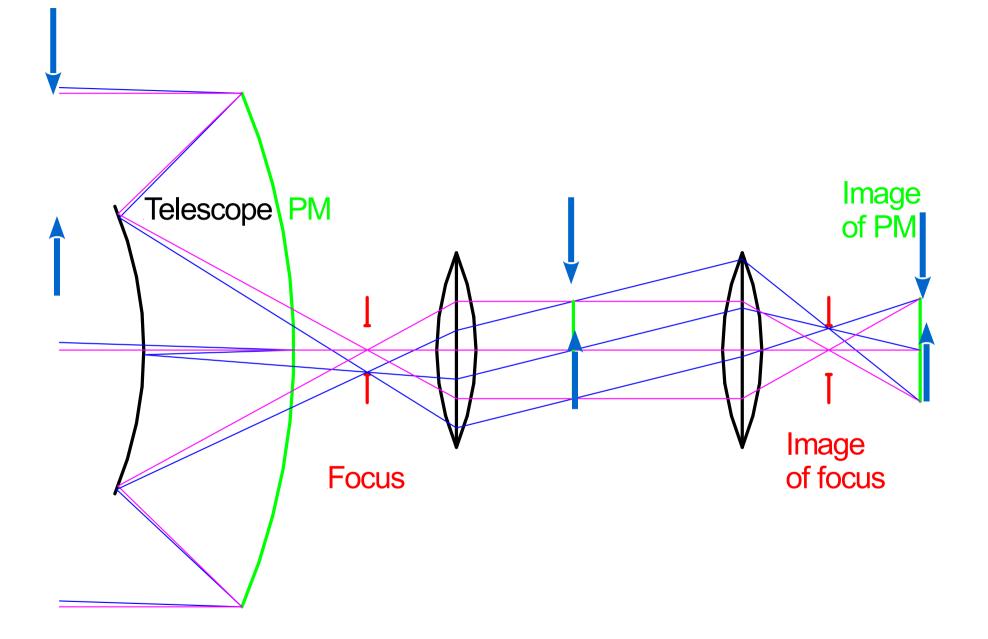
Trigger delay measurement





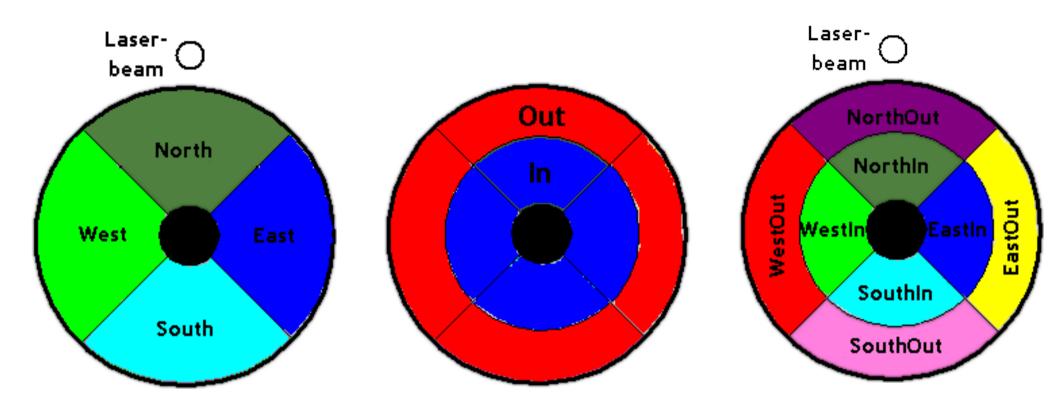




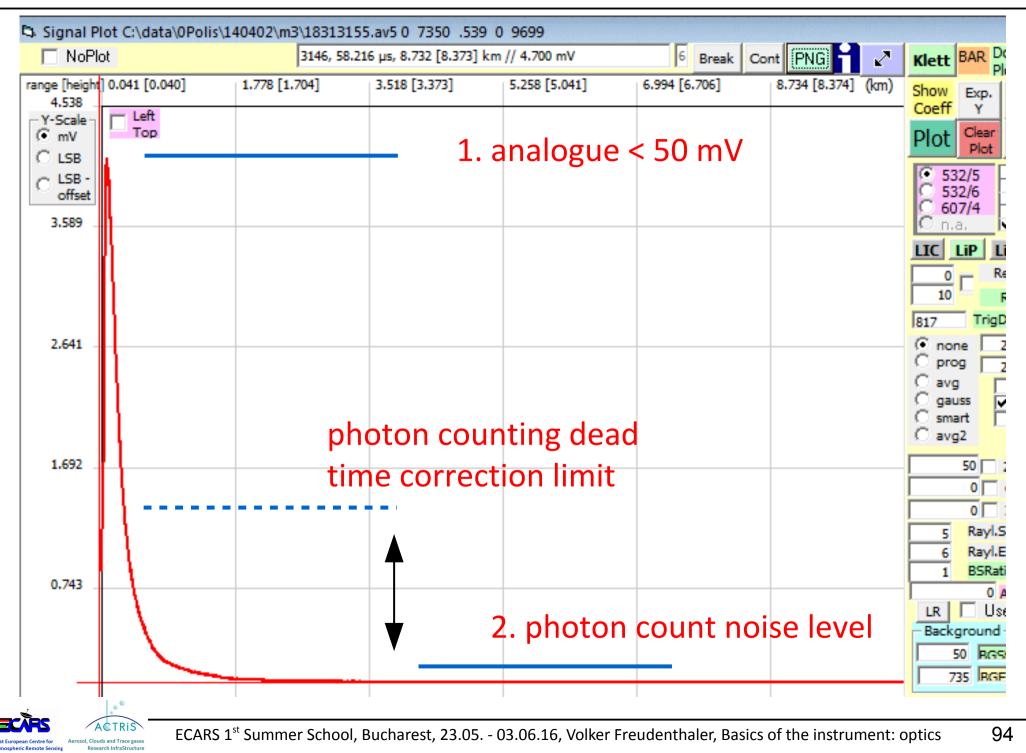




Telecover measurements







Signal limits

CONTROLLING STRESS IN BONDED OPTICS

Andrew Bachmann, Dr. John Arnold and Nicole Langer DYMAX Corporation, Torrington, Connecticut October 1, 2001

delamination, birefringence can lead to optical failure. Figure 4, below shows a photograph of birefringence caused by the adhesive at three stress points. The birefringence radiates out from the stress points from a positioning adhesive as seen through a polarizer. Figure 5 shows adhesive-caused stress in a doublet boned over the entire lens surface.

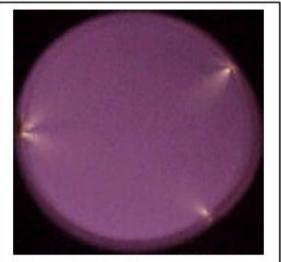


Figure 4. Birefringence as seen through a polariscope at each of a 3-point bond for a 1 inch diameter optic

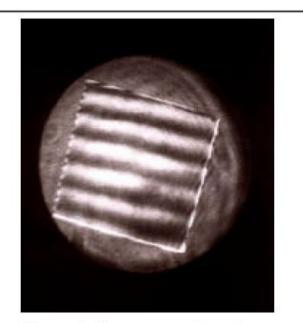


Figure 5. Lens, as seen through a polarized film

